

1 **Response to Review**

2
3 We thank the referees for their comments on our paper. We have responded to all the
4 referee comments through the responses below and through modifications to our manuscript.
5 This process has improved our manuscript, which we hope is now suitable for publication. To
6 guide the review process, referee comments are in plain text, our responses are in italics,
7 additions to our manuscript are shown below in red and as tracked changes in the revised
8 manuscript.

9
10 As a result of the reviewer comments regarding AOD, we have made improvements to the
11 way in which we calculate AOD from the model output. We now calculate the AOD assuming
12 internally mixed aerosol, which is more consistent with our modelling approach in GLOMAP.
13 We also found that the way in which the extinction was calculated previously was not
14 consistent with our modelling approach. Extinction efficiency from only one aerosol
15 component was being used in the calculation of AOD rather than the extinction for each
16 specific aerosol component. Correcting this in the code, substantially improved our simulated
17 AOD values relative to the observations (with both the external and internal mixing
18 assumptions). We have updated statistical values and figures in the manuscript and altered
19 the description of the AOD calculation in the text to describe the revised method assuming
20 internal mixing (please see the revised manuscript for details).

21
22 We have now also included additional sensitivity tests in the paper for the AOD calculation,
23 testing the assumptions of mixing (internal versus external) and calculation of water uptake.
24 Please see the responses to individual reviewer comments below and the revised manuscript
25 for further detail.

26 27 28 **Anonymous Referee #1**

29
30 The paper of Reddington et al. investigates the impacts of biomass burning on tropical
31 aerosols. This is done with GLOMAP global aerosol model, evaluated by long-term surface
32 observation of PM_{2.5} and AOD. Specifically, this work compares three different fire emission
33 datasets (GFED3, GFAS1 and FINN) to explore the uncertainty in emissions.

34
35 This study aims to “better understand the discrepancy in modeled biomass burning
36 AOD and to ultimately improve estimates of biomass burning aerosol”. While the authors
37 address the contribution of underestimation in biomass burning aerosols to the bias in AOD,
38 it would have been beneficial if they could perform further analysis to see the relative
39 contribution of other factors. For example, if they assume internal mixing instead of external
40 mixing, what does this do to the modeled AOD bias? Is the uncertainty in RH large enough to
41 explain the bias in modeled AOD?

42
43 *We agree that these are important next steps. However, further isolating the reason for*
44 *model bias will be very difficult without additional observations. In future work we are using*
45 *detailed observations of the vertical profile of aerosol and relative humidity to better*
46 *understand the causes for model bias. We hope that this future work will allow us to explore*
47 *the contribution of different factors to model bias, including the uncertainty in RH as*
48 *suggested by the referee.*

49
50 *As suggested, we have tested the sensitivity of internal versus external mixing in our*
51 *calculation of AOD. We have included an addition figure (Fig. 7 in the revised manuscript)*
52 *and added the following text to Section 4.1.3:*

53

1 “We find that the difference in AOD between assuming an external mixture of aerosol species and an
2 internal (volumetrically-averaged) mixture is limited. Figure 7 shows the simulated versus observed
3 multi-annual monthly mean AOD at AERONET sites when assuming external and internal mixing and
4 indicates that the difference is less than 5%, internal mixing generally yielding higher AOD at the
5 AERONET site locations. However, we note that the internal mixing assumption does not take into
6 account the lensing effects of coating BC with organic aerosol, which has been shown to interact with
7 the aerosol absorption in a non-linear way (Saleh et al., 2015).”

8 *We have also included an additional test to estimate the sensitivity of the simulated AOD to*
9 *the calculated hygroscopic growth of the aerosol (please see Section 4.1.3 in the revised*
10 *manuscript).*

11 In summary, this paper is well written. It describes what they did and is easy to follow along.
12 It adds value to the literature on this topic and is worthy of publication in ACP subject to
13 addressing these.

14 *We thank the referee for these positive comments.*

16 **Other minor things:**

- 17 1. Are the model results also obtained for the year of 2003-2011? I did not see it in the
18 text.

19 *Yes, we have now clarified this in the text (P6, L24-25, revised manuscript):*

20 “Simulations were run for the period 2003 to 2011.”

- 21 2. I found it difficult to read the titles for x/y axis and legend in figure 4&8.

22 *We will ensure that the axes titles and legends are legible in the ACP version of our paper.*

25 **Anonymous Referee #2**

27 **General comments**

28
29 The paper evaluates multi-annual (2003-2011) monthly mean values of near-surface aerosol
30 mass concentration (PM_{2.5}) and aerosol optical depth (AOD) simulated by the GLOMAP
31 global aerosol model against corresponding measurements conducted at four ground
32 stations in the Amazon region and at 27 AERONET stations located in tropical regions
33 worldwide. The simulations were done with three different datasets of biomass burning
34 emissions (GFED3, FINN1, and GFAS1). Additional numerical experiments involved scaling
35 the biomass burning emissions by a factor of 1.5 or 3.4. The model performance is evaluated
36 in terms of the Pearson correlation coefficient and the normalized mean bias factor (NMBF).
37 It is found that the model considerably underestimates both PM_{2.5} concentrations and AOD,
38 with a greater underestimation of AOD than PM_{2.5}. The paper is well written and the
39 presentation quality is good. However, the scientific significance and the overall scientific
40 quality of the study are questionable.

41
42 Indeed, the fact that models tend to underestimate AOD over regions affected by fires
43 (including the Amazon region) is well known. This is acknowledged by the authors: some
44 earlier studies reporting the underestimation of AOD are mentioned in the paper, although
45 the list of such studies is certainly not complete (see also, e.g., Petrenko et al., 2012;
46 Konovalov et al., 2014). The use of ground measurements of surface aerosol mass
47 concentration together with AOD measurements is a relatively novel point. However, the

1 parallel analysis of PM_{2.5} and AOD measurements, as well as the use of three different
2 emission datasets also did not help to fully explain the mismatch between the model and
3 measurements of AOD. Note that Petrenko et al. (2012) has presented a much more
4 extensive analysis of the impact of biomass burning emission.

5
6 *We agree with the referee that a novelty in our analysis is using surface PM_{2.5}*
7 *concentrations in addition to AOD. We also agree that whilst our study does not fully explain*
8 *the discrepancy between model and measured AOD, it provides additional evidence for*
9 *potential reasons. In future work we aim to exploit extensive observations of aerosol*
10 *properties from the SAMBBA field campaign over the Amazon to further explore this issue.*
11 *We thank the reviewer for pointing us to these additional papers which are now cited in the*
12 *revised manuscript.*

13
14 A serious drawback of the analysis is that it is based on an obsolete / simplistic
15 understanding of organic aerosol processes. In particular, the authors disregard the well-
16 established facts that organic aerosol (which is a major fraction of biomass burning aerosol)
17 is formed by organic compounds featuring a broad distribution of volatilities (see, e.g., May et
18 al., 2013) and that a part of them, while in the gas phase, can provide a major source of
19 secondary organic aerosol (SOA) (see, e.g., Grieshop et al., 2009; Hennigan et al., 2011) as
20 a result of oxidation processes. Meanwhile, these facts have direct implications for biases in
21 biomass burning aerosol emission inventories and for the mismatch between simulations and
22 measurements of AOD (Jathar et al., 2014; Konovalov et al., 2015; Shrivastava et al., 2015).
23 Although it is briefly mentioned that the SOA formation in biomass burning plumes can
24 contribute to the difference between the simulations and observations, any quantitative
25 estimates of such a contribution are not provided. A study could benefit from simulations of
26 biomass burning aerosol by using the volatility basis set framework and available
27 parameterizations (e.g., Hodzic et al., 2010; Shrivastava et al., 2013, 2015). In any case,
28 simplifications made in the model in regard to organic aerosol processes (such as an implicit
29 assumption that organic part of biomass burning aerosol consist only of non-volatile material)
30 and their implications for the results of this analysis had to be carefully described and
31 discussed in light of earlier findings from relevant laboratory, field and modeling studies.

32
33 *We thank the reviewer for these comments. We agree with the referee that including a*
34 *treatment of SOA formation from biomass burning may be important. To address this we*
35 *have extended our discussion of SOA formation in biomass burning plumes. Implementing a*
36 *volatility basis set (VBS) algorithm into global aerosol microphysics models is difficult due to*
37 *the large number of additional tracers this requires, as well as large parameter uncertainty.*
38 *For this reason very few global aerosol microphysics models have implemented such a*
39 *complex treatment of organic aerosol. Our treatment of organic aerosol is similar to many*
40 *other global aerosol microphysics models (Tsigaridis et al., 2014), making our model*
41 *appropriate for exploring the ability of such models to simulate organic aerosol in regions*
42 *influenced by biomass burning. We note that global models with greater complexity in their*
43 *treatment of organic aerosol do not necessarily better simulate observed organic aerosol*
44 *(Tsigaridis et al., 2014).*

45
46 *As suggested by the referee, we have added a discussion of how the treatment of organic*
47 *aerosol may impact our results. We have added text in the introduction:*

48
49 *“The contribution of secondary organic aerosol (SOA) from the oxidation of volatile organic*
50 *compounds in biomass burning plumes is also a large uncertainty (Jathar et al., 2014; Shrivastava et*
51 *al., 2015).”*

52
53 *as well as in Section 4.1:*

54

1 “In future work we need to include the formation of semi-volatile SOA in biomass burning plumes
2 that has been shown to be important (Konovalov et al., 2015; Shrivastava et al., 2015).”

3
4 *and the conclusions:*

5
6 “We have treated biomass burning emissions as primary and non-volatile. Formation of semi-volatile
7 SOA in biomass burning plumes may be important (Konovalov et al., 2015; Shrivastava et al., 2015)
8 and needs to be explored in future work.”

9
10
11 **Specific comments**

- 12
13 1. Page 6. The PM_{2.5} measurements made by the gravimetric filter analysis method
14 that is known to be associated with large uncertainties (Malm et al., 2011). The
15 authors estimate uncertainties of such measurements to be 15%. But how was the
16 loss of organic aerosol mass due to desorption estimated? Available volatility
17 distributions of fresh biomass burning emissions (e.g., May et al., 2013) imply that the
18 loss of the organic aerosol mass from samples taken inside biomass burning plumes
19 (POM~1000 ug/m³) after equilibration to ambient conditions (POM~10 ug/m³) could
20 be as large as 40 percent.

21 *We agree with the reviewer that the filter measurements used in our paper are associated*
22 *with uncertainties and subjected to positive biases (mostly due to water) and negative biases*
23 *(volatilization of semivolatile organics). Aerosols could volatilize along the filter exposure due*
24 *to ambient temperature variations. Fortunately, in Amazonia the diurnal variation of*
25 *temperature is relatively low (<~3°C), which helps to limit volatilization. In addition, before*
26 *gravimetric analysis, the filters are kept at controlled conditions of 20°C and 50% RH. This*
27 *temperature of 20°C is usually below the temperature at which the samples were taken (25.2*
28 *± 1.6°C annual mean in Porto Velho), which also helps to prevent volatilization.*

29 *At the current time, we do not have means to quantify the losses due to volatilization as done*
30 *by Malm et al. (2011), because the system used was simpler compared to the system used*
31 *by the IMPROVE network. What we can do are mass reconstructions and also comparisons*
32 *between filter-based PM_{2.5} and particle mass derived from other measurements, such as*
33 *size distribution, AMS measurements and BC measurements. Such comparisons yielded the*
34 *15% uncertainty estimate stated in the paper.*

35 *Regarding the loss of POM from fresh biomass burning plumes, the filter measurements*
36 *were not intended to accurately describe PM_{2.5} concentrations close to the biomass burning*
37 *source, but instead intended to describe the variability of PM_{2.5} concentrations at*
38 *Amazonian sites impacted by already aged biomass burning plumes (aging of 3-12 h,*
39 *depending on the site and on the distribution of fire spots).*

- 40 2. Page 9, line 12. The fire emissions were injected into the model by using a set of
41 fixed ecosystem-dependent altitudes. Meanwhile, it is known that the injection height
42 depends on the fire intensity. If, for example, the injection height for major fires was
43 underestimated in the model, the surface PM_{2.5} concentration during fire seasons
44 could be overestimated. The study could benefit from using one of more realistic
45 parameterizations of the injection height (e.g., Sofiev et al., 2012; Paugam et al.,
46 2016). And, anyway, it would be important to ensure by means of a sensitivity
47 analysis that the discrepancies between the results obtained with PM_{2.5} and AOD
48 measurements are not due to biases in the injection height. The adequacy of the
49 injection heights could further be evaluated by using surface measurements of CO
50 concentrations and satellite observations of CO columns (see, e.g., Konovalov et al.,
51 2014).

1 This is a good suggestion and would be interesting to explore in future work. However,
2 including a plume rise parameterization in our model would be a substantial piece of
3 research that is not possible in our present study. We also note that using a plume rise
4 model does not always lead to improved agreement with observations in biomass burning
5 regions (e.g. Archer-Nicholls et al., 2015).

6 Extensive efforts to constrain fire injection heights have been described elsewhere and are
7 not a specific focus of this work. We add the following text to Sect. 3.1:

8 “Analysis of smoke plume heights has demonstrated that most smoke emissions from fires occur
9 within the boundary layer (Val Martin et al., 2010).”

10 References:

11 Archer-Nicholls, S., Lowe, D., Darbyshire, E., Morgan, W. T., Bela, M. M., Pereira, G.,
12 Trembath, J., Kaiser, J. W., Longo, K. M., Freitas, S. R., Coe, H., and McFiggans, G.:
13 Characterising Brazilian biomass burning emissions using WRF-Chem with MOSAIC
14 sectional aerosol, *Geosci. Model Dev.*, 8, 549-577, doi:10.5194/gmd-8-549-2015, 2015.

15 Val Martin, M., Logan, J. A., Kahn, R. A., Leung, F.-Y., Nelson, D. L. and Diner, D. J.:
16 Smoke injection heights from fires in North America: Analysis of 5 years of satellite
17 observations, *Atmos. Chem. Phys.*, 10, 1491–1510, doi:10.5194/acp-10-1491-2010, 2010.

18 3. Page 10, line 13. "The water uptake for each soluble aerosol component is calculated
19 on-line in the model according to ZSR theory". Was hygroscopicity of organic
20 components of biomass burning aerosol taken into account in the simulations? If so,
21 what were typical values of the hygroscopic growth factor for the organic fraction?

22 Yes, the hygroscopicity of organic components of biomass burning aerosol is taken into
23 account in the simulations. The water content of each mode in GLOMAP given component
24 concentrations (in air) is calculated using ZSR and binary molalities evaluated using water
25 activity data from Jacobson (2005; Table B.10, p. 748). The particulate organic matter (POM)
26 component is assumed to be water-insoluble in the insoluble mode but is assumed to have
27 aged chemically in the aerosol to become hygroscopic once transferred to the soluble
28 modes. To represent this in the ZSR calculation, the aged POM component is assumed to
29 take up water at a fraction (set at 0.65) of sulphate.

30 We have added the following text to Section 3.2:

31 “The water uptake for each soluble aerosol component is calculated on-line in the model according to
32 Zdanovskii-Stokes-Robinson (ZSR) theory, which estimates the liquid water content as a function of
33 solute molarity (Stokes and Robinson, 1966). We assign moderate hygroscopicity to POM in the
34 soluble modes, consistent with a water uptake per mole at 65% of SO₄ (Mann et al., 2010).”

35 References:

36 Jacobson, M. Z. (2005), *Fundamentals of Atmospheric Modeling*, 2nd Edn, Cambridge
37 University Press.

38 Stokes, R. H. and Robinson, R. A.: *Interactions in aqueous nonelectrolyte solutions. I.*
39 *Solute-solvent equilibria*, *J. Phys. Chem.*, 70, 2126–2130, 1966.

40 4. Section 3.3. The paper could significantly benefit from an analysis of inter-annual
41 variability of fire emissions and of corresponding PM_{2.5}/AOD values in the Amazon
42 region during the fire season. Has such a variability been predicted by the different
43 inventories consistently? Can the model reproduce the observed inter-annual
44 variability in PM_{2.5}? Which of the inventories considered does enable the best
45 agreement between the inter-annual variations in the simulations and measurements
46 of PM_{2.5}?

47 These are good suggestions but would add substantially to what is already a long paper.
48 Analysis of inter-annual variability is not a specific focus of this piece of work. Also, the

1 reason for calculating and comparing average seasonal cycles is that we were keen to
2 ensure that the number of data points at each observation site would be equal so that the
3 overall statistical values would not be biased by model performance at one or two locations
4 with more years of data available.

5 In order to evaluate the model's and emission datasets' abilities to reproduce the observed
6 inter-annual variability, we have included additional figures in the supplementary material
7 (Figs. S2 and S3) to show the modelled versus observed annual mean PM2.5 concentrations
8 and AOD. We have also added the following text to Sect. 4.1.1:

9 “If we consider the inter-annual variability in simulated and observed PM2.5 concentrations (Figure
10 S2), we find that the results are consistent with the evaluation of the simulated seasonal cycle. The
11 smallest bias between model and observations is with the FINN1 emissions (NMBF= -0.22) compared
12 to GFED3 (NMBF= -0.36) or GFAS1 (NMBF= -0.48). One notable point is that the model with
13 GFED3 emissions simulates the highest PM2.5 concentrations for the 2010 drought year, relative to
14 the model with GFAS1 or FINN1 emissions, leading to improved agreement with observations at
15 Porto Velho (see Figs. 3a, 4a and S2).”

16 5. Page 15, line 17. "This suggests that the negative model bias in the dry season is
17 largely due to uncertainty in the biomass burning emissions rather than
18 anthropogenic emissions, SOA or microphysical processes in the model." Please see
19 above a general comment about the potential importance of SOA formation in
20 biomass burning plumes.

21 We have reworded this statement to clarify we mean biogenic SOA:

22 “This suggests that the negative model bias in the dry season is largely due to uncertainty in the
23 biomass burning rather than anthropogenic emissions, biogenic SOA or microphysical processes in the
24 model.”

25 6. Page 20, line 20. "Uncertainties exist in the calculation of AOD that may contribute to
26 the negative bias in simulated AOD." Did the authors try to validate their AOD
27 calculations with other independent data? For example, it would be interesting to see
28 if the model calculations are consistent with available measurements of the mass
29 scattering and absorbing efficiencies (e.g. Reid et al., 2005). A bias in these
30 parameters would indicate a similar bias in the AOD calculations.

31 This is a good suggestion. However, there are a number of difficulties involved in comparing
32 simulated values with the measurements in Reid et al. (2005). Firstly, the mass absorbing
33 efficiencies (MAEs) obtained by Reid and Hobbs (1998) were for fires observed in the 1995
34 burning season; we only have GFED3, GFAS1 and FINN1 model simulations for the 2003-
35 2011 period, where burning conditions may be quite different to those observed in 1995.
36 Secondly the measured values are for smoke less than 4 minutes old, which a global model
37 is unlikely to be able to capture. For these reasons we have included a comparison between
38 the simulated and observed values rather than a detailed evaluation. We have also included
39 a comparison between the GLOMAP simulated values with those of other models. We have
40 added the following to the supplementary material:

41 “Reid and Hobbs (1998) report values of mass absorption efficiency (MAE) for smouldering ($0.7 \pm 0.1 \text{ m}^2 \text{ g}^{-1}$)
42 and flaming ($1.0 \pm 0.2 \text{ m}^2 \text{ g}^{-1}$) forest fires in Brazil, sampled between 13th August and 25th September
43 1995. To evaluate the simulated mass extinction efficiency (MEE) against observations, we calculated
44 values of MEE from the observed MAE and single scattering albedo (SSA) from Reid and Hobbs (1998),
45 assuming: $\text{MAE} = \text{MEE} * (1 - \text{SSA})$. For smouldering forest fires we obtained an “observed” MEE (550 nm)
46 of $4.4 \text{ m}^2 \text{ g}^{-1}$ (range: 3.3 to $5.7 \text{ m}^2 \text{ g}^{-1}$, calculated from the quoted standard errors). To compare to the
47 observed value, we calculated MEEs at 550 nm for each simulation (with fire emissions), in grid cells that
48 cover the locations where smoke from the forest fires were sampled (in the vicinity of Porto Velho,
49 Rondônia and Marabá, Pará), and calculated an average for August over the period 2003-2011.

1 The average simulated MEE values of 5.2-5.4 m² g⁻¹ (using the ZSR water uptake scheme to calculate
2 aerosol hygroscopic growth) and 3.4-3.5 m² g⁻¹ (using the κ-Köhler water uptake scheme) span the
3 observed value and are within the uncertainty range of the observations. The range in the simulated values
4 (e.g. 5.18-5.35 m² g⁻¹) demonstrates the relatively limited sensitivity of the MEE to the fire emission
5 dataset (average values are within 5%) compared to the sensitivity to the calculation of aerosol hygroscopic
6 growth (with average values differing by a factor of 1.5). The comparison between simulated and observed
7 MEEs supports the conclusion in the main text (Sect. 4.1.3) that the ZSR and κ-Köhler AOD are likely to
8 represent high and low water uptake cases, respectively.

9 We also compare the GLOMAP simulated global mean values for aerosol burden, AOD, and MEE against
10 those of other global aerosol models (see Table S2). In general we find that the GLOMAP global mean
11 aerosol burdens and AOD (550 nm) are consistent with values from AEROCOM (Kinne et al., 2006) and
12 Heald et al. (2014) for SO₄, BC and sea salt. For the POM and mineral dust components, both the burden
13 and AOD are underestimated by GLOMAP relative to the other models. There could be several reasons for
14 this underestimation (including different anthropogenic emissions and/or aerosol removal schemes in the
15 models), but one factor that may partly explain the higher burden and AOD values for POM from the
16 GEOS-Chem model relative to GLOMAP is the higher assumed POM:OC ratio of 2 (Heald et al., 2014),
17 compared to 1.4 assumed in GLOMAP. The GLOMAP simulated global mean MEEs for all components
18 are within the large range in values reported by AEROCOM (Kinne et al., 2006; Mhyre et al., 2013) and
19 Heald et al. (2014). The MEEs for POM, SO₄ and BC calculated using the ZSR water uptake scheme are
20 generally at the upper end of the AEROCOM values (particularly for BC), and those calculated using the κ-
21 Köhler water uptake scheme are towards the lower end.”

22 *References added:*

23 *Heald, C. L., Ridley, D. A., Kroll, J. H., Barrett, S. R. H., Cady-Pereira, K. E., Alvarado, M. J.,*
24 *and Holmes, C. D.: Contrasting the direct radiative effect and direct radiative forcing of*
25 *aerosols, Atmos. Chem. Phys., 14, 5513-5527, doi:10.5194/acp-14-5513-2014, 2014.*

26 *Kinne, S., Schulz, M., Textor, C., Guibert, S., Balkanski, Y., Bauer, S. E., Berntsen, T.,*
27 *Berglen, T. F., Boucher, O., Chin, M., Collins, W., Dentener, F., Diehl, T., Easter, R.,*
28 *Feichter, J., Fillmore, D., Ghan, S., Ginoux, P., Gong, S., Grini, A., Hendricks, J., Herzog, M.,*
29 *Horowitz, L., Isaksen, I., Iversen, T., Kirkevåg, A., Kloster, S., Koch, D., Kristjansson, J. E.,*
30 *Krol, M., Lauer, A., Lamarque, J. F., Lesins, G., Liu, X., Lohmann, U., Montanaro, V., Myhre,*
31 *G., Penner, J., Pitari, G., Reddy, S., Seland, O., Stier, P., Takemura, T., and Tie, X.: An*
32 *AeroCom initial assessment – optical properties in aerosol component modules of global*
33 *models, Atmos. Chem. Phys., 6, 1815–1834, doi:10.5194/acp-6-1815-2006, 2006.*

34 *Myhre, G., Samset, B. H., Schulz, M., Balkanski, Y., Bauer, S., Berntsen, T. K., Bian, H.,*
35 *Bellouin, N., Chin, M., Diehl, T., Easter, R. C., Feichter, J., Ghan, S. J., Hauglustaine, D.,*
36 *Iversen, T., Kinne, S., Kirkevåg, A., Lamarque, J. F., Lin, G., Liu, X., Lund, M. T., Luo, G.,*
37 *Ma, X., van Noije, T., Penner, J. E., Rasch, P. J., Ruiz, A., Seland, O., Skeie, R. B., Stier, P.,*
38 *Takemura, T., Tsigaridis, K., Wang, P., Wang, Z., Xu, L., Yu, H., Yu, F., Yoon, J. H., Zhang,*
39 *K., Zhang, H., and Zhou, C.: Radiative forcing of the direct aerosol effect from AeroCom*
40 *Phase II simulations, Atmos. Chem. Phys., 13, 1853–1877, doi:10.5194/acp-13-1853-2013,*
41 *2013.*

42 *Reid, J. S. and Hobbs, P. V.: Physical and optical properties of smoke from individual*
43 *biomass fires in Brazil, J. Geophys. Res., 103, 32 013–32 031, 1998.*

45 **Minor comments**

- 46
47 1. Page 11, line 17. Daily GFED3 fire emissions were implemented in GLOMAP for the
48 period 2003–2011, with monthly emissions implemented for the period 1997–2002.
49 Were simulations analyzed in this paper really extended to the period 1997–2002?

50 *We only analyse model simulations for 2003-2011, so we have removed the statement*
51 *discussing simulations for 1997-2002 (which were only performed with GFED3 emissions).*
52 *We have clarified the simulation period in the text (P6, L24-25, revised manuscript):*

1 “Simulations were run for the period 2003 to 2011.”

2 *and (P9, L9-10, revised manuscript):*

3 “We complete GLOMAP simulations for the period 2003 to 2011 where all three emission datasets are
4 available.”

5 2. Several papers cited in the text (Chin et al., 2009; Randerson et al., 2012; Zhou et al.
6 2002 : :) are missing in the references.

7 *Thank you for spotting this. We have added these papers to the references and have*
8 *carefully checked that all cited papers are now included in the reference list.*

9

10 **Anonymous Referee #3**

11

12 This manuscript evaluates global aerosol model simulations that have been performed with
13 the GLOMAP model and three widely used fire emission inventories, namely GFED3, GFAS1
14 and FINN1. The simulations are validated thoroughly and in considerable detail with AOD
15 and PM2.5 measurements performed in the tropics, i.e. South America, Africa and SE Asia.
16 The study addresses the most pertinent issues recently discussed in the field of smoke
17 aerosol modelling, i.e. the omission of small fires in burnt-area-based inventories and the
18 need to scale up the pyrogenic aerosol flux for use in global atmospheric models. The
19 statistical analysis is based on monthly mean values. The study is therefore very well suited
20 as a guide on how to best select one of the fire emission inventories for use with GLOMAP,
21 and on how accurate the simulated smoke AOD and PM2.5 may be. Considering the wide
22 use of GLOMAP and of the investigated emission inventories, the study presents relevant
23 results that are worth publication in ACP.

24

25 *We thank the referee for these positive comments on our manuscript.*

26

27 The study is well written and clearly presented. It adds quantitative detail to the already
28 existing characterization of the fire emission inventories. However, this quantitative detail
29 appears to be linked to using the GLOMAP model, and it cannot necessarily be transferred to
30 use in other atmospheric aerosol models. The authors missed several opportunities to obtain
31 more generally applicable new results. In particular:

32

- 33 • Correlations are calculated from monthly averages like so many studies have done in
34 the past. Since emission, model and observation data are available with daily
35 resolution, investigating this time scale would have been easily possible and much
36 more novel.

37 *This is a good suggestion. However, most of the aerosol observations are not available*
38 *consistently at 24-hour resolution, but are often averages over several days (see Page 6,*
39 *Line 15-16, ACPD version). Thus a detailed comparison at daily time resolution is not*
40 *possible with this dataset.*

41

42 *We have, however, put a lot of effort into performing a more accurate comparison between*
43 *than model and observations than simply comparing monthly means. Prior to calculating the*
44 *monthly averages, we removed all invalid or missing observation ‘days’ from the model time-*
45 *series. In addition, if the PM2.5 measurement extended over a period of more than 1 day*
46 *then we averaged the model data over same number of days. Therefore, the model and*
47 *observed monthly means are calculated over the same days in each month. This is*
48 *particularly important when considering the model evaluation against AERONET AOD, since*
49 *the Level 2 AERONET data contain numerous gaps in the time-series. In future work we will*
50 *evaluate the model at sub-monthly time scales where we have observations consistently*
51 *available at higher time resolution.*

1
2 To give a qualitative comparison between model and observations at higher than monthly
3 time resolution, we have included a additional figure in the supplementary material (Figure
4 S1) showing the full time series (between 2003 and 2011) of un-averaged observed PM2.5
5 concentrations with daily modelled PM2.5 concentrations.
6

- 7 • The study shows that PM2.5 and AOD require different upscaling of emissions. It
8 would have been most interesting and new to study possible reasons for this. I
9 suspect, it points to model shortcomings, but in which part of the model?
- 10 • Likewise, it would have been of general interest to see whether any of the model
11 configuration parameters have an impact on the amount of upscaling required for any
12 given inventory.
13

14 We agree that these are important next steps. However, it is difficult to make progress on this
15 issue without additional observations. In future work we are using detailed aircraft
16 observations of the vertical profile of aerosol combined with ground and satellite AOD and
17 the model to further explore model deficiencies and isolate the probable cause.
18

19 Now that we have improved the calculation of AOD, we find that the model biases in PM2.5
20 and AOD are more consistent in South America, although not at every location. To
21 investigate this discrepancy further, we have performed some additional sensitivity studies
22 with the simulated AOD. We tested the sensitivity of simulated AOD to assumptions about
23 the aerosol mixing state and hygroscopic growth. We find that the simulated AOD is very
24 sensitive to the calculation of water uptake, which could have a large impact on the amount
25 of upscaling of emissions required for the model match observed AOD. This highlights how
26 the use of an emissions scaling factor could be compensating for inadequate understanding
27 of water uptake by the aerosol and the subsequent changes in aerosol size distribution and
28 optics.

29 I am aware that addressing one of these issues in the final manuscript will imply a major
30 effort, which may not be justified at this stage. However, if the authors would be willing to do
31 it, this would certainly make the results applicable for a much larger community, i.e. also
32 those who use other models than GLOMAP or its results.
33

34 Since the manuscript is very well written, I have only very few minor comments:
35

36 **SPECIFIC COMMENTS**

- 37
38 1. p.11, l.1 and p.12, l.13: delete “yearly varying”

39 Deleted as suggested.

- 40 2. p.11, l.28: You may cite Seiler Crutzen 1980 for this formula.

41 Done.

- 42 3. p.14, l.16: Please add the definition of NMBF when first using it for the convenience of
43 the general reader.

44 We have added the following to Sect.4.1.1:

45 “To quantify the agreement between model and observations, we use the Pearson correlation
46 coefficient (r) and normalised mean bias factor (NMBF) as defined by Yu et al. (2006):

$$NMBF = \frac{(\sum M_i - \sum O_i)}{|\sum M_i - \sum O_i|} \left[\exp \left(\left| \ln \frac{\sum M_i}{\sum O_i} \right| \right) - 1 \right]$$

47 where M and O represent the multi-annual monthly mean model and observed values, respectively, for
48 each month i . A positive NMBF indicates the model overestimates the observations by a factor of

1 NMBF+1. A negative NMBF indicates the model underestimates the observations by a factor of 1–
2 NMBF.”

3 4. p.20, l.17-17: Here you first discuss the influence of the model resolution on the
4 representativity of the station observations. This is not linked to the next sentence,
5 which raises the question the resolution’s influence on the need for scaling. This is an
6 example for my second point made above.

7 *We have assumed this comment refers to P20, L19-24 (ACPD version). This is a good point*
8 *and we agree that the two issues have been conflated in this paragraph, although we do*
9 *believe the two issues are linked. We acknowledge that a relatively coarse model resolution*
10 *presents a limitation in the comparison with point measurements. However, we do interpolate*
11 *the model values to the specific site locations so we have altered the paragraph in question*
12 *to focus more on the potential for model resolution to decrease agreement at the sites (rather*
13 *than how well the site location represents the surrounding area):*

14 “Another important factor that will also influence the calculated AOD is the spatial resolution of the
15 simulated aerosol and RH (used to calculate aerosol water uptake) fields. These fields are on a
16 relatively coarse spatial resolution and will not capture small scale (sub-grid) variability in these
17 quantities that may influence point location measurements from AERONET stations. A higher
18 resolution model would be required to test how sensitive the simulated AOD is to the spatial resolution
19 of the aerosol and RH fields and whether or not increasing the resolution improves the agreement with
20 observed AOD (and reduces the discrepancy between the model performance in AOD and PM2.5).
21 Bian et al. (2009) showed that increasing the resolution of the RH field from 2°x2.5° to 1°x1.25° can
22 increase the simulated AOD by ~10% in biomass burning regions (improving agreement with
23 observations), which may partly explain the larger discrepancies in AOD than PM2.5.”

24 *Reference added: Bian, H., Chin, M., Rodriguez, J. M., Yu, H., Penner, J. E., and Strahan,*
25 *S.: Sensitivity of aerosol optical thickness and aerosol direct radiative effect to relative*
26 *humidity, Atmos. Chem. Phys., 9, 2375-2386, doi:10.5194/acp-9-2375-2009, 2009.*

27 5. Figure 9: It would help to print the scaling factor also in the graphics and you may
28 consider merging this with Figure 3 to make the comparisons easier for the reader.

29 *Thank you for this suggestion. Figures 3 and 9 and figures 6 and 10 have now been merged*
30 *and labels added.*

31
32

33 REFERENCES

34 W. Seiler, P. J. Crutzen. Estimates of gross and net fluxes of carbon between the
35 biosphere and the atmosphere from biomass burning. Climatic Change, 2(3):207–247,
36 1980.

37

38 **Please find the full revised manuscript on the following pages. Significant changes to**
39 **the manuscript (and those in response to the reviewer comments above) are shown**
40 **with tracked changes. Minor editorial or grammatical corrections have not been**
41 **tracked.**

42

43

1

2 **Analysis of particulate emissions from tropical biomass**
3 **burning using a global aerosol model and long-term**
4 **surface observations**

5 **C.L.Reddington¹, D.V. Spracklen¹, P. Artaxo², D.A. Ridley^{1,3}, L.V. Rizzo⁴ and A.**
6 **Arana²**

7 [1] {School of Earth and Environment, University of Leeds, Leeds, United Kingdom}

8 [2] {Department of Applied Physics, Institute of Physics, University of Sao Paulo, Sao Paulo,
9 Brazil}

10 [3] {now at Department of Civil and Environmental Engineering, Massachusetts Institute of
11 Technology, USA}

12 [4] {Institute of Environmental, Chemical and Pharmaceutical Sciences, Federal University of
13 Sao Paulo, Diadema, Brazil}

14 Correspondence to: C. L. Reddington (c.l.s.reddington@leeds.ac.uk)

15

16 **Abstract**

17 We use the GLOMAP global aerosol model evaluated against observations of surface
18 particulate matter (PM_{2.5}) and aerosol optical depth (AOD) to better understand the impacts
19 of biomass burning on tropical aerosol over the period 2003 to 2011. Previous studies report a
20 large underestimation of AOD over regions impacted by tropical biomass burning, increasing
21 particulate emissions from fire by up to a factor 6. To explore the uncertainty in emissions we
22 use three satellite-derived fire emission datasets (GFED3, GFAS1 and FINN1) in the model,
23 in which tropical fires account for 66-84% of global particulate emissions from fire. The
24 model underestimates dry season PM_{2.5} concentrations ~~where observations are available in~~
25 regions of high fire activity in South America and underestimates AOD over South
26 America, Africa and Southeast Asia. Underestimation of AOD over tropical regions impacted
27 by biomass burning is slightly reduced, relative to ~~consistent with~~ previous studies. Where
28 coincident observations of surface PM_{2.5} and AOD are available we find a greater model
29 underestimation of AOD than PM_{2.5} at some sites. Increasing particulate emissions to

1 improve simulation of AOD can therefore lead to overestimation of surface PM2.5
2 concentrations. With FINN1 emissions increased by a factor of 1.5 the model reasonably
3 simulates PM2.5 concentrations and AOD in South America and AOD over Southeast Asia,
4 but underestimates AOD over ~~South America and~~ Africa. The model with GFAS1 emissions
5 better matches observed PM2.5 and AOD when emissions are increased by a factor of 3.4,
6 with the exception of Equatorial Asia where a scaling factor of 1.5 is adequate. The model
7 with GFED3 emissions increased by a factor of 1.5 reasonably simulates PM2.5
8 concentrations and AOD in active deforestation regions in South America and AOD in
9 Equatorial Asia, but requires a larger scaling factor to capture observed AOD in Africa,
10 Indochina and elsewhere in South America~~in all regions~~. The model with GFED3 emissions
11 poorly simulates observed seasonal variability of surface PM2.5 and AOD in regions where
12 small fires dominate, providing independent evidence that GFED3 omits emissions from
13 small fires. Seasonal variability of both PM2.5 and AOD in South America is better simulated
14 by the model using FINN1 and GFAS1 emissions. Detailed observations of the vertical
15 profile of aerosol over biomass burning regions are required to better constrain emissions and
16 modelled AOD.

17

18 **1. Introduction**

19 Open biomass burning is an important source of trace gases and particulate matter (PM) to the
20 atmosphere (Crutzen and Andreae, 1990; Andreae and Merlet, 2001; Van der Werf et al.,
21 2010). Biomass burning emissions can influence weather (Kolusu et al., 2015; Gonçalves et
22 al., 2015; Tosca et al., 2015) and climate (Ramanathan et al., 2001; Tosca et al., 2013;
23 Jacobson, 2014) directly, by scattering and absorbing solar radiation (Johnson et al., 2008;
24 Sakaeda et al., 2011), and indirectly, by modifying cloud properties (Andreae et al., 2004;
25 Feingold et al., 2005; Tosca et al., 2014). The influence of biomass burning aerosol on surface
26 radiation can have subsequent impacts on the biosphere. For example, smoke plumes from
27 biomass burning have been observed to increase plant productivity, through increasing the
28 amount of diffuse radiation (Oliveira et al., 2007; Doughty et al., 2010), which has been
29 shown to be a regionally important process over the Amazon (Rap et al., 2015). PM from
30 biomass burning can substantially degrade regional air quality leading to adverse effects on
31 human health (Emmanuel, 2000; Frankenberg et al., 2005; Johnston et al., 2012; Jacobson,
32 2014; Reddington et al., 2015). A better understanding of particulate emissions is needed to
33 improve predictions of the impacts on biomass burning on climate and air quality. Here we

1 use a global aerosol model with tropical observations of surface PM and aerosol optical depth
2 (AOD) to better understand the impact of tropical fires on atmospheric aerosol.

3 The spatial and temporal distribution of fires depends on climate, vegetation and human
4 activities. At the global scale, fire emissions are dominated by burning in the tropics (van der
5 Werf et al., 2010). Anthropogenic activity can increase the occurrence of fires either directly,
6 through deforestation fires and agricultural residue burning (van der Werf et al., 2010), or
7 indirectly, through land-use/land-cover change that acts to increase the fire susceptibility of
8 the land surface e.g. forest fragmentation in the Amazon (Cochrane and Laurance, 2002) and
9 large-scale drainage of peatlands in Indonesia (Field et al., 2009; Carlson et al., 2012). Human
10 activity can also reduce the occurrence of fires, directly through fire suppression and
11 indirectly through reducing and fragmenting fuel loads which limits fire spread (Birstinas et
12 al., 2014). Over the 21st century, predicted changes in rainfall and temperature may increase
13 forest water stress and subsequent fire occurrence in tropical forests (Cox et al., 2008;
14 Golding and Betts, 2008; Malhi et al., 2009). The incidence of fire and resulting emissions are
15 therefore sensitive both to changing climate and changes in land-use (Heald and Spracklen,
16 2015).

17 High temporal and spatial variability in biomass burning emissions coupled with the
18 difficulties involved in conducting measurements in remote tropical regions lead to major
19 challenges for their quantification. In recent years, global estimates of biomass burning
20 emission fluxes have mostly been obtained using satellite remote sensing (e.g., van der Werf
21 et al., 2006, 2010; Reid et al., 2009; Wiedinmyer et al., 2011; Kaiser et al., 2012; Zhang et al.,
22 2012; Ichoku and Ellison, 2014), which provides long-term observations with relatively high
23 spatial coverage. A range of satellite products and methods are utilised to derive fluxes of
24 aerosol and gas-phase species emitted from fires. The most common methods use satellite-
25 retrieved burned area, active fire counts, and/or fire radiative power (FRP) in combination
26 with biogeochemical models (when using burned area) and/or species-specific emission
27 factors obtained from laboratory experiments and field observations (e.g., Hoelzemann et al.,
28 2004; Ito and Penner, 2004; 2005; van der Werf et al., 2006, 2010; Wiedinmyer et al., 2006;
29 2011; Schultz et al., 2008; Kaiser et al., 2012). Large uncertainties are associated with
30 satellite observations of fires and with the various methods used to calculate emissions fluxes
31 from the observational data (e.g. Ito and Penner, 2005; Reid et al., 2009; [Kononov et al.,](#)
32 [2014](#))

1 Previous studies using satellite-derived emissions and atmospheric models to investigate the
2 properties and impacts of biomass burning aerosol have found a persistent underestimation of
3 AOD observed in most tropical biomass burning regions (Matichuk et al., 2007; 2008; Chin et
4 al., 2009; [Petrenko et al., 2012](#); Kaiser et al., 2012; Ward et al., 2012; Tosca et al., 2013). In
5 general, modelling studies have required biomass burning emissions or concentrations of
6 biomass burning aerosol to be increased by factors ranging from ~1.5 to ~6 in order to match
7 satellite and ground based observations of AOD (Matichuk et al., 2007; 2008; Johnson et al.,
8 2008; Sakaeda et al., 2011; Johnston et al., 2012; Kaiser et al., 2012; Tosca et al., 2013;
9 Marlier et al., 2013). The underestimation of AOD observed in biomass burning regions has
10 been attributed to a number of factors (see e.g., Kaiser et al., 2012) including: i)
11 underestimation of biomass burning emission fluxes; ii) errors in modelling the atmospheric
12 distribution and properties of biomass burning aerosol; and iii) uncertainties in the calculation
13 of AOD.

14 Uncertainties associated with the derivation of emission fluxes arise from errors present in the
15 satellite-detection of active fires or burned area (e.g. obscuring of the surface by clouds and
16 smoke, satellite spatial resolution and detection limits, and satellite overpass time), as well as
17 uncertainties in emission factors and fuel consumption estimates. For example, Randerson et
18 al. (2012) suggest that emission datasets based on relatively coarse burned area data
19 (detection limit of ~100 Ha), result in an underestimation of global area burned by ~35%,
20 although this error is not sufficient to fully explain the underestimation of AOD discussed
21 above. Inadequate representation of biomass burning aerosol in models, including errors in
22 the modelled aerosol size distribution, chemical composition, ageing processes, vertical and
23 horizontal transport (including fire emission injection heights) and dry/wet removal from the
24 atmosphere, could also contribute to an underestimation of AOD. [The contribution of
25 secondary organic aerosol \(SOA\) from the oxidation of volatile organic compounds in
26 biomass burning plumes is also a large uncertainty \(Jathar et al., 2014; Shrivastava et al.,
27 2015\).](#) In the calculation of AOD itself, the uncertainties associated with the assumed optical
28 properties of biomass burning aerosol e.g. their refractive indices, hygroscopicity (uptake of
29 water onto the aerosol), and/or mixing state (i.e. treated as core/shell mixtures,
30 internally/externally mixed etc.) may also contribute to this negative model bias in AOD.

31 Using only AOD to evaluate estimates of biomass burning aerosol emissions can be
32 misleading because AOD depends on many factors in addition to aerosol abundance. Scaling
33 biomass burning emissions to match observed AOD could therefore lead to inaccurate model

1 representation of biomass burning aerosol concentrations and, subsequently, errors in model
2 predictions of the air quality and climate effects of biomass burning aerosol. Although there
3 has been extensive use of AOD retrievals to evaluate model predictions of biomass burning
4 aerosol, thus far there have been relatively few studies to use aerosol measurements to
5 thoroughly evaluate these models (e.g., Liousse et al., 2010; Daskalakis et al., 2015).

6 In this study, we evaluate a global aerosol microphysics model against observations of aerosol
7 mass concentrations in addition to AOD to better understand the discrepancy in modelled
8 biomass burning AOD and to ultimately improve estimates of biomass burning aerosol. We
9 also compare three different biomass burning emission inventories to investigate regional
10 differences between emissions and identify the best fit emissions for future modelling studies.

11

12 **2. Observations**

13 To evaluate the simulated distribution of PM at the surface, we use long-term *in-situ*
14 measurements of PM_{2.5} (particulates with aerodynamic diameters < 2.5 μm) mass
15 concentrations conducted at four ground stations in the Amazon region (Alta Floresta, Porto
16 Velho, Santarem and Manaus; ~~detailed in Table S1 in the supplementary material~~). The
17 location and observation period are detailed for each station in Table S1 in the supplementary
18 material. Figure S1 shows the measured PM_{2.5} concentrations at each station between 2003
19 and 2011, demonstrating the data coverage.

20 The PM_{2.5} measurements were made using gravimetric filter analysis and the measurement
21 duration ranges from less than 1 day to more than 10 days. Particles were sampled under
22 ambient relative humidity (RH) conditions (typically in the range of 80-100% RH). The
23 sampled filters were weighed after 24 hours of equilibration at 50% RH and 20°C. Amazonian
24 submicrometer aerosol particles have growth factors of ~1.1-1.3 at 90% RH (Zhou et al, 2002;
25 Rissler et al., 2006) so we estimate that water represents roughly ~10-20% of the PM_{2.5} mass
26 concentrations at measurement conditions. Uncertainties related to filter handling, sampling
27 and analysis are estimated as 15% of particle mass. Further information on the measurements
28 conducted at the Manaus and Porto Velho stations can be found in Artaxo et al. (2013). Our
29 evaluation of PM_{2.5} is restricted to Amazonia since there are few long-term observations of
30 PM_{2.5} in other tropical regions impacted by biomass burning.

31 The measurement stations at Porto Velho and Alta Floresta are located in the arc of
32 deforestation and are strongly impacted by fresh biomass burning emissions (Fig. 1). The

1 Santarem and Manaus stations are located within forest reservations and are impacted by
2 transported regional biomass burning emissions in the dry season. The Santarem station is
3 located in Para, where the number of fire hotspots observed by satellites during the dry season
4 are typically a factor of ~10 greater than the number observed in Amazonas, where the Manaus
5 station is located. Thus in the dry season, PM_{2.5} concentrations measured at Santarem are
6 typically higher than those measured at Manaus.

7 To evaluate the simulated distribution of AOD, we use observations of spectral columnar
8 AOD measured by the Aerosol Robotic Network (AERONET) using ground-based Cimel sun
9 photometers (Holben et al., 1998). Specifically, we use Level 2.0 (quality assured) daily
10 average AOD retrieved at 440 nm from 27 AERONET stations detailed in Table S1. We
11 selected stations located within regions influenced by tropical biomass burning (Southeast and
12 Equatorial Asia, Central and Southern Africa, and the Amazon region in South America) that
13 have more than one year of relatively continuous data (automatic cloud screening leads to
14 gaps in the dataset) between 2003 and 2011. We note that whilst the majority of cloud-
15 contaminated AOD data is removed; comparisons with co-located Micro-Pulse Lidar Network
16 observations indicate that some contamination from thin cirrus clouds may remain, possibly
17 leading to small positive biases in observed AOD (Huang et al., 2011; Chew et al., 2011).

18 To compare modelled and observed PM_{2.5} and AOD, daily-mean model output was linearly
19 interpolated to the location (latitude, longitude and altitude above sea level) of each ground
20 station. Model data that corresponded to gaps in the observation datasets were removed prior
21 to calculating monthly-mean values used in the analysis. The modelled PM_{2.5} concentration
22 is calculated for dry aerosol, omitting the contribution of water to the total mass, thus
23 modelled PM_{2.5} concentrations may be underestimated compared to the observations, which
24 include some contribution from the mass of water.

25

26 **3. Model description**

27 **3.1 Global aerosol microphysics model**

28 The global distribution of aerosol was simulated using the 3-D Global Model of Aerosol
29 Processes (GLOMAP; Spracklen et al., 2005a,b; Mann et al., 2010), which is an extension to
30 the TOMCAT chemical transport model (Chipperfield, 2006). Simulations were run for the
31 period 2003 to 2011. Large scale atmospheric transport and meteorology in TOMCAT are

1 specified from European Centre for Medium-Range Weather Forecasts (ECMWF) analyses,
2 updated every 6 hours and linearly interpolated onto the model time-step. The model runs at a
3 horizontal resolution of $2.8^{\circ} \times 2.8^{\circ}$ with 31 vertical model levels between the surface and 10
4 hPa. The vertical resolution in the boundary layer ranges from ~60 m near the surface to ~400
5 m at ~2 km above the surface. GLOMAP has been extensively evaluated in previous studies
6 against aerosol observations (Mann et al., 2010, 2014; Spracklen et al., 2011a,b; Browse et
7 al., 2012; Schmidt et al., 2012; Scott et al., 2014; Reddington et al., 2011, 2013, 2014). Below
8 we describe the features of the model relevant for this study, please see Spracklen et al.
9 (2005a) and Mann et al. (2010) for more detailed descriptions of the model.

10 GLOMAP simulates the mass and number of size resolved aerosol particles in the
11 atmosphere, including the influence of aerosol microphysical processes on the particle size
12 distribution. These processes include nucleation, coagulation, condensation, ageing,
13 hygroscopic growth, cloud processing, dry deposition, and nucleation/impact scavenging. The
14 aerosol particle size distribution is represented using a two-moment modal scheme with seven
15 log-normal modes (Mann et al., 2010). Within each mode, aerosol particles are treated as
16 internally mixed. GLOMAP treats the following aerosol species: black carbon (BC),
17 particulate organic matter (POM), sulphate (SO_4), sea spray and mineral dust. Biogenic SOA
18 is formed in the model via the reaction of biogenic monoterpenes with O_3 , OH and NO_3 ,
19 which produces a gas-phase oxidation product that condenses with zero vapour pressure onto
20 pre-existing aerosol (Spracklen et al., 2006, 2008). Concentrations of oxidants are specified
21 using monthly-mean 3-D fields at 6-hourly intervals from a TOMCAT simulation with
22 detailed tropospheric chemistry (Arnold et al., 2005) linearly interpolated onto the model
23 time-step. Monthly mean emissions of biogenic monoterpenes are taken from the Global
24 Emissions Initiative (GEIA) database (Guenther et al., 1995). Size-resolved emissions of
25 mineral dust are prescribed from daily-varying emissions fluxes provided for AEROCOM
26 (Dentener et al., 2006).

27 For this study, anthropogenic emissions of sulphur dioxide (SO_2), BC and organic carbon
28 (OC) ~~POM~~ were specified using the MACCity emissions inventory (Lamarque et al., 2010;
29 Granier et al., 2011), which provides annually varying emissions for the period 1979-2010.
30 For simulations in the year 2011 we used MACCity anthropogenic emissions from 2010.
31 Biomass burning emissions of SO_2 , BC and ~~POM-OC~~ were specified using three different
32 satellite-derived emission datasets, which are described in detail in Section 3.3. We convert
33 OC to POM using a prescribed POM:OC ratio of 1.4, which is at the lower end of the range

1 | [prescribed in other global models \(1.4 to 2.6\) \(Tsigaridis et al., 2014\)](#). The fire emissions were
2 | injected into the model over six ecosystem-dependent altitudes between the surface and 6 km
3 | recommended by Dentener et al. (2006). In the regions studied in this paper (South America,
4 | Africa and Southeast Asia), the fire emission injection heights range between the surface and
5 | an altitude of ~3 km asl. The largest fraction of the fire emissions, ranging from ~99% of
6 | emissions in Equatorial Asia to 88% in Indochina, are injected below 1 km asl (or at surface
7 | level if the altitude of the model level exceeds 1 km asl). [Analysis of smoke plume heights](#)
8 | [has demonstrated that most smoke emissions from fires occur within the boundary layer \(Val](#)
9 | [Martin et al., 2010\)](#).

10 | Primary carbonaceous aerosol particles [are assumed to be non-volatile and](#) are emitted into
11 | the model with a fixed log-normal size distribution, assuming a number median diameter of
12 | 150 nm for biomass burning emissions and 60 nm for fossil fuel emissions and modal width
13 | (σ) of 1.59. Several previous studies have investigated the impacts of the uncertainty in the
14 | assumed emission size distribution on simulated aerosol and cloud condensation nuclei
15 | concentrations (Pierce et al., 2007; Pierce and Adams, 2009; Reddington et al., 2011; 2013;
16 | Lee et al., 2013) and aerosol radiative forcing (Bauer et al., 2010; Spracklen et al., 2011b;
17 | Carslaw et al., 2013). An assumption of a number median diameter of 150 nm for biomass
18 | burning emissions is reasonably consistent with measurements of the size distributions of
19 | fresh biomass burning aerosol from grassland (100 – 125 nm) and deforestation (100 – 130
20 | nm) fires (Reid et al., 2005 and references therein). Once emitted into the model, the
21 | components of primary carbonaceous aerosol (BC and OC) are assumed to mix
22 | instantaneously and are initially treated as non-hygroscopic. Once these particles have
23 | accumulated 10 monolayers of soluble material (assumed to be SOA and H₂SO₄) through
24 | condensation, they are transferred directly to the corresponding soluble Aitken or
25 | accumulation mode to account for ageing. [For a discussion of the treatment of organic aerosol](#)
26 | [within global aerosol models see Tsigaridis et al. \(2014\)](#).

27 | **3.2 Calculation of aerosol optical depth**

28 | AOD was calculated from the simulated aerosol size distribution using Mie theory assuming
29 | spherical particles (Grainger et al., 2004) that are externally mixed within each log-normal
30 | mode. For this study, modelled AOD was calculated at a wavelength of 440 nm using
31 | component-specific refractive indices at the closest wavelength available (468 nm) from
32 | Bellouin et al. (2011). Water uptake plays a significant role in determining AOD, altering the

1 refractive index and the size distribution of the aerosol. The water uptake for each soluble
2 aerosol component is calculated on-line in the model according to [Zdanovskii-Stokes-](#)
3 [Robinson \(ZSR\) theory, which estimates the liquid water content as a function of solute](#)
4 [molarity \(Stokes and Robinson, 1966\). We assign moderate hygroscopicity to POM in the](#)
5 [soluble modes, consistent with a water uptake per mole at 65% of SO₄](#) (Mann et al., 2010).
6 The resulting daily-mean wet radii and refractive indices are used to calculate the daily-mean
7 aerosol extinction. Using hourly-mean values of water uptake increased simulated daily AOD
8 on average by less than 1%.

9 **3.3 Biomass burning emissions**

10 In this study we compare three different satellite-derived datasets of biomass burning
11 emissions: the Global Fire Emissions Database version 3 (GFED3; van der Werf et al., 2010),
12 the National Centre for Atmospheric Research Fire Inventory version 1.0 (FINN1;
13 Wiedinmyer et al., 2011) and the Global Fire Assimilation System version 1.0 (GFAS1;
14 Kaiser et al., 2012). The key aspects of these emission inventories are summarised in Table 1.
15 [We complete GLOMAP simulations for the period 2003 to 2011 where all three emission](#)
16 [datasets are available.](#)

17 GFED3 provides monthly-mean fire emissions of aerosol and gas-phase species from 1997 to
18 2011 at 0.5°×0.5° resolution (van der Werf et al., 2010). GFED3 emissions are derived using
19 the monthly-mean time series of global burned area estimates from Giglio et al. (2010). For
20 1997-2000, the fire emissions are based on burned area derived from the TRMM Visible and
21 Infrared Scanner (VIRS) and Along-Track Scanning Radiometer (ATSR) active fire data and
22 estimates of plant productivity derived from observations from the Advanced Very High
23 Resolution Radiometer (AVHRR). For November 2000 onwards, the fire emissions are based
24 on estimates of burned area, active fire detections, and plant productivity from the MODerate
25 resolution Imaging Spectroradiometer (MODIS) instrument on-board the Terra and Aqua
26 satellites. To derive total carbon emissions the satellite datasets are combined with estimates
27 of fuel loads and combustion completeness for each monthly time step from the Carnegie-
28 Ames-Stanford-Approach biogeochemical model. The carbon emission fluxes are converted
29 to trace gas and aerosol emissions using species specific emission factors compiled by
30 Andreae and Merlet (2001). From 2003 onwards, GFED3 fire emissions are available on a
31 daily time step, developed using detections of active fires from MODIS (Mu et al., 2011).
32 Daily GFED3 fire emissions were implemented in GLOMAP for the period 2003-2011.

1 FINN1 provides daily fire emissions of aerosol and gas-phase species from 2002 to 2012 on a
2 1 km² grid (Wiedinmyer et al., 2011). FINN1 fire emissions are based on detections of active
3 fires (specifically their location and timing) from the MODIS Fire and Thermal Anomalies
4 Product (Giglio et al., 2003). FINN1 also uses the MODIS Land Cover Type product to
5 specify land cover classes and the MODIS Vegetation Continuous Fields product to identify
6 the fractions of tree and non-tree vegetation, and bare ground. Specifically, the emitted mass
7 (E) of a certain species (i) is calculated using the following equation [\(Seiler and Crutzen,](#)
8 [1980\)](#):

$$9 \quad E_i = A(x, t) \times B(x) \times FB \times ef_i \quad (1)$$

10 | Where ~~the~~ A is the area burned at time t and location x , B is the biomass loading at location x ,
11 FB is the fraction of that biomass that is burned and ef is the emission factor of species i . For
12 each fire count the area burned, A , is assumed to be 0.75 km² for fires detected on grassland
13 and savannah land cover classes, and 1 km² for those detected on all other land cover classes
14 following Wiedinmyer et al. (2006) and Al-Saadi et al. (2008). Adjustments are made to the
15 assumed burned area if the fire pixel extends partially over bare ground (reducing the burned
16 area by the percentage of bare area assigned to that pixel). Estimates of biomass loading, B ,
17 are taken from Hoelzemann et al. (2004) and are assumed to be land cover specific. The
18 fraction of biomass assumed to burn, FB , in each fire pixel is determined as a function of tree
19 cover using relationships from Ito and Penner (2004) (see Wiedinmyer et al., 2006). Emission
20 factors, ef , for each species are taken from Akagi et al. (2011).

21 GFAS1 provides daily fire emissions of aerosol and gas-phase species from March 2000 to
22 2013 at 0.5°×0.5° resolution (Kaiser et al., 2012). Like FINN1, GFAS1 uses the observed
23 geo-location of active fires from the MODIS instrument. However, GFAS1 also makes use of
24 the NASA fire products (MOD14 and MYD14) that provide quantitative information on the
25 radiative power of detected fires (Justice et al., 2002; Giglio, 2005). The FRP fields are
26 corrected for observation gaps due to partial cloud-cover by assuming the same FRP areal
27 density throughout the grid cell. Data assimilation is used to further fill observation gaps
28 using information from earlier FRP observations (see Kaiser et al., 2012). Spurious signals
29 from volcanoes, gas flares and other industrial activity are removed from the data. The FRP is
30 converted to the combustion rate of dry matter using land-cover-specific conversion factors
31 ~~derived by Heil et al. (2012)~~, based on data from GFED3 [\(Heil et al., 2010; Kaiser et al.,](#)
32 [2012\)](#). As for GFED3, species emission rates are calculated using updated emission factors
33 based on Andreae and Merlet (2001).

1 Table 1 gives the total annual amounts of BC and OC aerosol emitted from fires over the
2 tropics for each emission inventory. The total BC and OC emitted from fires in the tropics
3 make up 77-84% and 66-77%, respectively of the global total emissions. FINN1 has the
4 greatest tropical OC emission, with emissions being 47% greater than in GFAS1 and 30%
5 greater than GFED3. Emission of BC is more consistent, with FINN1 BC emissions being
6 13% greater than GFAS1 and 1% greater than GFED3. This results in different OC:BC
7 emission ratios between the datasets with the mean ratio across the tropics varying from 10.0
8 in FINN1, 7.9 in GFED3 and 7.1 in GFAS1.

9 Figure 1a-c shows the spatial distribution of annual total biomass burning emissions of OC
10 from each fire inventory averaged over the period of 2003 to 2011. There are similarities in
11 the general spatial distributions of fire emissions, with all three inventories showing
12 maximum emissions over the tropical savannah and humid subtropical regions of Africa, the
13 arc of deforestation in Amazonia, coastal regions of Indonesia (Sumatra and Kalimantan),
14 northern Australia, and parts of Indochina (particularly Cambodia, Laos and Myanmar).
15 However, Figs. 1d-f show that there are strong regional differences between the different
16 emission inventories. Differences between FINN1 and GFAS1 (Fig. 1e) and FINN1 and
17 GFED3 (Fig. 1f) are more spatially organised than differences between GFAS1 and GFED3
18 (Fig. 1d), which are more spatially heterogeneous.

19 Over Africa, GFED3 gives higher OC emissions in northern tropical savannah and southern
20 humid subtropical regions, with GFAS1 and FINN1 giving higher emissions than GFED3 at
21 the boundaries of these regions and over central Africa. Over Australia, GFED3 gives the
22 highest OC emissions estimates over the tropical savannah region of northern Australia, with
23 GFAS1 giving the highest emissions in the dryer grassland and desert regions further south.

24 Over South America the picture is more complex. In general, FINN1 and GFAS1 emission
25 estimates are higher in northern and eastern Brazil than GFED3, with GFAS1 giving the
26 highest emissions over eastern areas and FINN1 over northern Brazil. FINN1 emissions are
27 generally higher than GFAS1 and GFED3 over the central and southern Amazon region
28 (particularly over the state of Mato Grosso), Peru and generally over northern South America.
29 GFED3 emissions are higher than FINN1 and GFAS1 in northern parts of Bolivia and the
30 northern part of the state of Rondônia in the arc of deforestation.

31 Over South Asia, Indochina and Equatorial Asia, FINN1 gives higher emissions than both
32 GFED3 and GFAS, particularly over Bangladesh, Myanmar and Laos, with the exception of

1 the coastal peatland regions of Sumatra and Kalimantan where GFAS1 and GFED3 give
2 higher emissions than FINN1. The differences in emissions over Indonesia may be explained
3 by a potentially improved representation of tropical peat fire emissions in GFED3 and GFAS1
4 relative to FINN1 (Andela et al., 2013).

5

6 **4. Results**

7 **4.1 Overview of all comparisons**

8 **4.1.1 Particulate matter concentrations in the Amazon region**

9 Figure 2 shows simulated versus observed multi-annual monthly mean PM2.5 concentrations
10 at each of the four ground stations in the Amazon region (see Fig. 1 for site locations). To
11 quantify the agreement between model and observations, we use the Pearson correlation
12 coefficient (r) and normalised mean bias factor (NMBF) as defined by Yu et al. (2006):

$$NMBF = \frac{(\sum M_i - \sum O_i)}{|\sum M_i - \sum O_i|} \left[\exp \left(\left| \ln \frac{\sum M_i}{\sum O_i} \right| \right) - 1 \right]$$

13 where M and O represent the multi-annual monthly mean model and observed values,
14 respectively, for each month i . A positive NMBF indicates the model overestimates the
15 observations by a factor of $NMBF+1$. A negative NMBF indicates the model underestimates
16 the observations by a factor of $1-NMBF$.

17 Figure 2 demonstrates the important contribution of biomass burning to PM2.5 concentrations
18 across the region: there is a strong improvement in the agreement between model and
19 observations when biomass burning emissions are included in the model (Fig. 2b-d; NMBF =-
20 0.62 to -0.25, $r^2=0.77-0.83$) relative to the simulation without fire emissions (Fig. 2a; NMBF=
21 -1.85, $r^2=0.44$).

22 The overall bias between model and observations is smallest with FINN1 emissions (NMBF=
23 -0.25) compared to GFED3 (NMBF= -0.49) or GFAS1 (NMBF= -0.62), with simulated
24 monthly mean concentrations mostly within a factor of ~2 of the observations. The correlation
25 between model and observations across all sites is relatively similar between the three
26 emission datasets, with a slightly stronger correlation with GFED3 emissions ($r^2=0.83$)
27 compared to FINN1 ($r^2=0.77$) and GFAS1 ($r^2=0.79$).

1 The NMBF and correlation between model and observations are shown for the individual
2 stations in Fig. 3a. Correlations are calculated between simulated and observed multi-annual
3 monthly mean concentrations to evaluate the ability of the model to simulate seasonal
4 variability in aerosol. In general, the model with fire emissions overestimates observed PM2.5
5 concentrations at the forest site near Manaus (mean NMBF=0.57) but underestimates
6 observed PM2.5 concentrations at the sites that are more strongly impacted by biomass
7 burning (Porto Velho, Alta Floresta and Santarem; mean NMBF= -0.60). Figure 3
8 demonstrates that the relatively small bias with the FINN1 emissions in Fig. 2 is partly due to
9 an overestimation of PM2.5 concentrations at Manaus (NMBF=0.98), but also due to smaller
10 model biases at the three other sites (-0.51 to -0.11) compared to GFED3 (-0.76 to -0.48) and
11 GFAS1 (-1.26 to -0.39).

12 Figure 4 shows the multi-annual average seasonal cycle in observed and simulated PM2.5
13 concentrations at the four measurement sites [\(the full time-series at each site is shown in Fig.
14 S1 in the supplementary material\)](#). The model with biomass burning emissions simulates the
15 observed seasonal variability in PM2.5 concentrations over the Amazon region, characterised
16 by high concentrations in the local dry season (between ~June to ~December depending on
17 the site) and relatively low concentrations in the wet season. At Porto Velho, Santarem and
18 Alta Floresta, the model underestimates observed PM2.5 concentrations during the dry season
19 and has relatively good agreement during the wet season. This suggests that the negative
20 model bias in the dry season is largely due to uncertainty in the biomass burning emissions
21 rather than anthropogenic emissions, [biogenic](#) SOA or microphysical processes in the model.
22 The model overestimates PM2.5 concentrations observed at Manaus all year round, but
23 particularly during the dry season. This positive model bias may be due to several factors
24 including a possible overestimation of biogenic SOA over tropical forests and/or the model
25 resolution, which is not fully capturing the gradient in PM2.5 concentrations between the arc
26 of deforestation and the relatively undisturbed forest near Manaus.

27 In previous work we carried out a detailed model sensitivity analysis that accounted for the
28 uncertainty in the emissions (including biomass burning) and in the model processes such as
29 wet removal and dry deposition of aerosol (Lee et al., 2013). This analysis confirms that the
30 parametric uncertainty in modelled PM2.5 concentrations at these four stations is dominated
31 by the uncertainty in the biomass burning emissions flux in the dry season and by the yield of
32 [biogenic](#) SOA in the wet season, rather than the removal processes in the model.

1 Figure 4 demonstrates the differences in the spatial and temporal variability between the three
2 fire emission datasets, with different emissions capturing the observations better in different
3 months and locations. The model with GFED3 emissions captures the average seasonal
4 variability in PM_{2.5} observed at Alta Floresta (Fig. 4; $r^2=0.69$) and Porto Velho ($r^2=0.94$)
5 reasonably well. In particular, better simulating the peak in dry season concentrations at Porto
6 Velho than both FINN1 ($r^2=0.72$) and GFAS1 ($r^2=0.85$) emissions. However, PM_{2.5}
7 concentrations observed towards the end of the biomass burning season at Alta Floresta
8 (September – November) and Porto Velho (October – November) are not well captured by
9 GFED3 emissions, leading to larger biases at these sites (NMBF= -0.73 and -0.48,
10 respectively) than with FINN1 emissions (-0.51 and -0.41, respectively). At Santarem, the
11 model with GFED3 emissions underestimates observed PM_{2.5} concentrations throughout the
12 dry season, leading to a relatively large model bias and poor correlation with the observations
13 (NMBF= -0.76, $r^2=0.39$). Agreement with the observations at this site is improved with either
14 FINN1 (NMBF= -0.11, $r^2= 0.76$) or GFAS1 (NMBF= -0.39, $r^2= 0.75$) emissions (discussed
15 further in Sect. 4.2).

16 If we consider the inter-annual variability in simulated and observed PM_{2.5} concentrations
17 (Figure S2), we find that the results are consistent with the evaluation of the simulated
18 seasonal cycle. The smallest bias between model and observations is with the FINN1
19 emissions (NMBF= -0.22) compared to GFED3 (NMBF= -0.36) or GFAS1 (NMBF= -0.48).
20 One notable point is that the model with GFED3 emissions simulates the highest PM_{2.5}
21 concentrations for the 2010 drought year, relative to the model with GFAS1 or FINN1
22 emissions, leading to improved agreement with observations at Porto Velho (see Figs. 3a, 4a
23 and S2).

24 In summary, the model captures the seasonal cycle and inter-annual variability of observed
25 PM_{2.5} reasonably well at biomass burning influenced sites in the Amazon. However, the
26 model underestimates observed concentrations in the dry season suggesting that the biomass
27 burning aerosol emission fluxes in all three emission inventories (GFED3, FINN1, GFAS1)
28 may be underestimated.- We explore this further in Section 4.3.

29 **4.1.2 Aerosol optical depth in tropical biomass burning regions**

30 Figure 5 shows the simulated versus observed multi-annual monthly mean AOD at 440 nm at
31 each of the AERONET sites displayed in Fig. 1 (simulated and observed annual means are
32 compared in Fig. S3). Agreement between model and observed AOD is improved

1 | substantially when biomass burning emissions are included in the model (Fig 5; NMBF= -
2 | 0.40 to -0.18, $r^2=0.62-0.69$) compared to the simulation without fire emissions (NMBF= -
3 | 0.69, $r^2=0.22$). As for PM_{2.5}, the bias in AOD across all sites is smallest with the FINN1
4 | emissions (NMBF= -0.18) compared to GFED3 (NMBF= -0.34) or GFAS1 (NMBF= -0.40).
5 | The model with FINN1 emissions also shows slightly improved correlation with the
6 | observations ($r^2=0.69$) relative to GFED3 ($r^2=0.67$) and GFAS1 ($r^2=0.62$).

7 | Figure 6a shows the NMBF and correlation between simulated and observed multi-annual
8 | monthly mean AOD at the individual AERONET sites, grouped by region. In South America,
9 | the bias in modelled AOD is smallest with the FINN1 emissions (mean NMBF= -0.47)
10 | compared to GFED3 (-0.69) and GFAS1 (-0.89) emissions, which is consistent with
11 | comparisons between modelled and observed PM_{2.5} in Amazonia (Sect. 4.1.1). In Indochina,
12 | the model with FINN1 emissions also gives the smallest bias (mean NMBF= -0.02), relative
13 | to GFED3 (-0.21) and GFAS1 (-0.23). In Africa, the model bias is smallest with GFED3
14 | emissions (mean NMBF= -0.78) compared to GFAS1 (-0.90) and FINN1 (-0.96). In
15 | Equatorial Asia, the model bias is small and does not vary substantially between the different
16 | emission datasets (FINN: 0.02, GFAS: -0.01, GFED: -0.02). In terms of temporal agreement
17 | between model and observations, the correlation is noticeably stronger with GFED3 (mean r^2
18 | =0.52) in Africa and with FINN1 (mean $r^2=0.75$) in Indochina, relative to the other emission
19 | datasets.

20 | In general, the model with fire emissions captures the seasonal variability in observed AOD
21 | best in South America (mean $r^2=0.90$) and captures the magnitude of observed AOD best in
22 | Southeast Asia (Equatorial Asia: mean NMBF= -0.00; Indochina: mean NMBF= -0.14). The
23 | agreement between model and observations in Africa is relatively poor, with substantial
24 | underestimation of observed AOD (mean NMBF= -0.88). The negative model bias in Africa
25 | is unlikely to be solely due to an underestimation of biomass burning aerosol and is likely
26 | complicated by a contribution from dust (Pandithurai et al., 2001; Sayer et al., 2014;
27 | Cesnulyte et al., 2014; Queface et al., 2011). There is better agreement between the model and
28 | observed AOD at Ascension Island, which observes aged biomass burning aerosol from the
29 | African continent (Sayer et al., 2014), with all three emission inventories (mean NMBF= -
30 | 0.38, $r^2=0.84$). This suggests that the model is able to capture outflow of biomass burning
31 | emissions from Africa.

32 | At the South American sites located in regions of high biomass burning activity associated
33 | with deforestation fires (Abracos Hill, Rio Branco, Ji Parana SE and Alta Floresta), there is a

1 small improvement in the correlation with observed AOD with FINN1 ($r^2=0.96-0.98$) and
2 GFAS1 ($r^2=0.94-0.97$) emissions relative to GFED3 ($r^2=0.79-0.88$). At these sites, AOD
3 observed at the tail end of the biomass burning season (~October-November) is better
4 captured by GFAS1 and FINN1 than GFED3, leading to the improved correlation relative to
5 GFED3. The model with GFED3 is generally better able to capture observed AOD at the peak
6 of the biomass burning season (~August-September) than GFAS1 and FINN, which is largely
7 due to relatively high GFED3 emission estimates for the drought years 2007 and 2010 ([see](#)
8 [Fig. S1](#)). These results are consistent with comparisons with observed PM_{2.5} concentrations
9 at Porto Velho and Alta Floresta (Sect. 4.1.1).

10 At the AERONET sites located in Equatorial Asia and the Philippines (Singapore, Bandung,
11 Manila Observatory, ND Marbel Univ) an improved performance of either the GFAS1 or
12 GFED3 emission inventories may be expected over FINN1 (Andela et al., 2013) due to their
13 improved representation of tropical peatlands (in Indonesia and Malaysian Borneo) in their
14 biome maps (van der Werf et al., 2010). The agreement between AOD observed at Bandung,
15 Indonesia and the model is marginally improved with GFED3 (NMBF= -0.14, $r^2=0.52$) or
16 GFAS1 (NMBF= -0.15, $r^2=0.47$) relative to FINN1 (NMBF= -0.18, $r^2=0.34$). However, at the
17 other sites we find no strong indication of an improved performance with GFED3 (NMBF= -
18 0.06 to 0.13, $r^2=0.15-0.24$) or GFAS1 (NMBF= -0.03 to 0.14, $r^2=0.13-0.56$) relative to FINN1
19 (NMBF= 0.04 to 0.17, $r^2=0.16-0.42$). At most of these sites the model does not simulate a
20 strong contribution of biomass burning to AOD, likely due to their urban locations, which
21 may explain why we do not see a substantial difference in the performances of the three
22 emission datasets. Long-term ground-based retrievals of AOD located outside the influence of
23 urban environments are lacking in Equatorial Asia.

24 At the African AERONET sites, observed AODs are generally better captured by the model
25 with GFED3 emissions (mean NMBF= -0.78, $r^2=0.52$) than with FINN1 (mean NMBF= -
26 0.96, $r^2=0.35$) or GFAS1 (mean NMBF= -0.90, $r^2=0.41$) emissions. Andela et al. (2013)
27 report that the GFED3 emissions flux of carbon monoxide (CO) is higher than GFAS1 or
28 FINN1 for humid savannah regions, where the burned area product may observe more cloud
29 covered fires than active-fire detection. This feature may explain the improved simulation of
30 AOD with GFED3 over Africa. Andela et al. (2013) also report that the FINN1 emission
31 estimates of CO are lower than both GFED3 and GFAS1 in global savannah regions, with the
32 largest spatial deviation found in humid savannahs where fire size is large. This may suggest

1 that the assumed fire size in FINN1 for savannah fires (0.75 km^2) could be too small for
2 humid savannah fires in Africa, contributing to an underestimation of AOD in this region.

3 **4.1.3 Overview of PM2.5 and AOD evaluation**

4 In the previous sections we have evaluated the model against ground based observations of
5 PM2.5 and AOD. In general, we find that the model is negatively biased against observations
6 in regions strongly influenced by biomass burning. However, the model bias in surface PM2.5
7 concentrations is generally smaller than for AOD over South America, where observations of
8 both quantities are available ($\text{NMBF}_{\text{PM2.5}} = -1.85$ to -0.25 , $\text{NMBF}_{\text{AOD}} = -2.38$ to -0.40 ; see Figs.
9 2 and S4). If we compare average model biases (with fires) in multi-annual monthly mean
10 PM2.5 and AOD (for 2003-2004) at locations where AERONET stations are in close
11 proximity to the PM2.5 measurement stations, we find a larger model bias in AOD at
12 Santarem/Belterra ($\text{NMBF}_{\text{PM2.5}} = -0.61$, $\text{NMBF}_{\text{AOD}} = -1.15$), but the reverse at Alta Floresta
13 ($\text{NMBF}_{\text{PM2.5}} = -0.64$, $\text{NMBF}_{\text{AOD}} = -0.42$).

14 These results suggest that although the negative model bias in PM2.5 and AOD may be partly
15 due to an underestimation of biomass burning aerosol emissions (due to uncertainties
16 associated with fire detection and subsequent calculations of emission fluxes), there are likely
17 to be other factors contributing to the model discrepancy in AOD that do not affect modelled
18 surface PM2.5 concentrations. These factors include uncertainties in the calculation of AOD
19 that are largely associated with assumptions made about the aerosol optical properties
20 (assumed refractive indices), mixing state (external/internal mixing) and hygroscopic growth
21 of the aerosol. We investigate the sensitivity of simulated AOD to these assumptions below.

22 As described in Sect. 3.2, to calculate AOD at 440 nm we use component-specific refractive
23 indices from Bellouin et al. (2011) for a wavelength of 468 nm ($1.500 - 0.000i$ for POM and
24 $1.750 - 0.452i$ for BC). To test the sensitivity of AOD to the choice of refractive indices, we
25 applied the refractive indices tested by Matichuk et al. (2007) for smoke aerosol ($1.54 -$
26 $0.025i$ calculated by Haywood et al. (2003) for young smoke aerosol over southern Africa;
27 $1.51 - 0.024i$ and $1.52 - 0.019i$ retrieved by an AERONET station, Ndola in Zambia, located
28 close to smoke sources) to the BC and POM components in our model., We find that the
29 modelled AOD is relatively insensitive to the choice of complex refractive index within the
30 range of values tested here (altering the magnitude of AOD by less than 5%), which is in
31 agreement with Matichuk et al. (2007). Although the range of refractive indices tested is

1 relatively narrow (Matichuk et al., 2007), this result suggests that uncertainty in the assumed
2 refractive indices is unlikely to explain the discrepancy in modelled AOD.

3 We also find that the modelled AOD is fairly insensitive to the mixing state assumption, with
4 limited difference in AOD between assuming optical properties derived from an external
5 mixture of aerosol species and an internal (volumetrically-averaged) mixture. Figure 7 shows
6 the simulated versus observed multi-annual monthly mean AOD at AERONET sites when
7 assuming external and internal mixing and indicates that the difference is less than 5%,
8 internal mixing generally yielding higher AOD at the AERONET site locations. However, we
9 note that the internal mixing assumption used in this study does not take into account the
10 lensing effects of coating BC with organic aerosol, which has been shown to interact with the
11 aerosol absorption in a non-linear way (Saleh et al., 2015).

12 As described in Sect. 3.2, the hygroscopic growth of the aerosol is calculated in the model
13 using the ZSR scheme. To test the sensitivity of AOD to aerosol hygroscopic growth, we
14 instead use the κ -Köhler water uptake scheme, based upon the Köhler equation with a single
15 hygroscopic parameter, κ , defining the water uptake for different chemical species (Petters
16 and Kreidenweis, 2007) (see description of method in Sect. S1 of the supplementary
17 material). For the SO_4 , sea spray and POM components in the model we used the mean values
18 of κ for ammonium sulphate, sodium chloride and organic aerosol for subsaturated air masses
19 (0.53, 1.12 and 0.07, respectively) from Petters and Kreidenweis (2007). BC is considered
20 entirely hydrophobic in this model when using this scheme. The κ value for POM is based
21 upon that of α -pinene six hours after emission and is likely to be a minimum value as
22 oxidation of organic aerosol as it ages will tend to increase the hygroscopicity further. A wide
23 range of κ values are reported in the literature for organic aerosol (~0.01-0.6; Petters and
24 Kreidenweis, 2007) and biomass burning particles (0.02-0.8; DeMott et al., 2009; Petters et
25 al., 2009).

26 Using the κ -Köhler scheme the water uptake is reduced relative to the ZSR scheme; reducing
27 the simulated AOD on average by a factor of 1.7 at AERONET sites (see Fig. 7). This large
28 reduction relative to ZSR is in part from the assumption that the SO_4^{2-} component behaves as
29 ammonium sulphate rather than the more hygroscopic sulphuric acid, and the reduced water
30 uptake for POM. Therefore, the ZSR and κ -Köhler AOD can be considered high and low
31 water uptake cases, respectively, and highlight the large uncertainty present in the AOD from
32 aerosol hygroscopicity. This result is confirmed by comparing simulated AOD and mass

1 extinction efficiencies for the two water uptake cases against observations and values from
2 other global aerosol models (see Sect. S2 and Table S2).

3 Another important factor that will also influence the calculated AOD is the spatial resolution
4 of the simulated aerosol and RH (used to calculate aerosol water uptake) fields. These fields
5 are on a relatively coarse spatial resolution and will not capture small scale (sub-grid)
6 variability in these quantities that may influence point location measurements from
7 AERONET stations. A higher resolution model would be required to test how sensitive the
8 simulated AOD is to the spatial resolution of the aerosol and RH fields and whether or not
9 increasing the resolution improves the agreement with observed AOD (and reduces the
10 discrepancy between the model performance in AOD and PM2.5). Bian et al. (2009) showed
11 that increasing the resolution of the RH field from 2°x2.5° to 1°x1.25° can increase simulated
12 AOD by ~10% in biomass burning regions (improving agreement with observations), which
13 may partly explain the larger discrepancies in AOD than PM2.5.~~whether or not the spatial~~
14 ~~resolution of the model contributes to the underestimation of observed AOD.~~

15 Errors may also exist in the model representation of biomass burning aerosol, for example in
16 the modelled particle size distribution, that the simulated PM2.5 concentrations will be
17 relatively insensitive to but that will have implications for the simulated optical properties of
18 the aerosol and thus affect the calculated AOD. In addition, since AOD is a column-integrated
19 quantity, an underestimation of AOD may be due to an underestimation of aerosol
20 concentrations aloft since we have shown that the model agrees relatively well with PM2.5
21 concentrations observed at the surface.

22 Further uncertainties in the model representation of biomass burning aerosol are associated
23 with the conversion of OC to organic matter (OM), which would affect both PM2.5
24 concentrations and AOD predicted by the model. Increasing the assumed OM:OC ratio would
25 increase the total simulated mass of biomass burning aerosol. In our model we assume a
26 relatively low OM:OC ratio of 1.4 compared to previous studies on biomass burning aerosol.
27 Kaiser et al. (2012) use a value of 1.5, but note this ratio is low compared to values of around
28 2.2 proposed for aged pollution and biomass burning aerosols by Turpin and Lim (2001),
29 Pang et al. (2006) and Chen and Yu (2007) and a value of 2.6 used by Myhre et al. (2003) for
30 biomass burning aerosol in southern Africa. These larger OM:OC ratios could account for in-
31 plume (sub-grid) atmospheric oxidation and subsequent SOA formation observed in some
32 biomass burning plumes (Vakkari et al., 2014). In future work we need to include the

1 [formation of semi-volatile SOA in biomass burning plumes that has been shown to be](#)
2 [important \(Konovalov et al., 2015; Shrivastava et al., 2015\).](#)

3 **4.2 Small-scale fires**

4 The GFED3 fire emissions are known to underestimate contributions from small-scale fires
5 (smaller than ~100 ha) that are below the detection limit of the global burned area product
6 derived from MODIS (Randerson et al., 2012). However, many of these small fires generate
7 thermal anomalies that can be detected by satellites (Randerson et al., 2012). This means that
8 fire inventories using active fire detections to derive emissions (FINN1 and GFAS1) will
9 better capture these small fires (Kaiser et al., 2012). Kaiser et al. (2012) demonstrate that
10 GFAS1 includes emissions from small fires that are omitted in GFED3. Some of the
11 differences between the spatial patterns of emissions seen in Fig. 1 are likely due to missing
12 small fires in GFED3.

13 This result is corroborated by our comparisons between modelled and observed PM_{2.5}
14 concentrations at Santarem in the north region of Brazil (Sect. 4.1.1), where the poor
15 agreement between the observations and model with GFED3 emissions (NMBF= -0.76,
16 $r^2=0.39$) is substantially improved by using either of the active-fire based emission inventories
17 (FINN: NMBF= -0.11, $r^2= 0.76$; or GFAS: NMBF= -0.39, $r^2= 0.75$). Randerson et al. (2012)
18 show that in the region surrounding the Santarem station there is a particularly high small fire
19 fraction of total burned area, which explains why the GFED3 emissions do not capture the
20 observations in this region of Brazil. This result is consistent with comparisons between
21 modelled and observed AOD at the nearby AERONET station, Belterra. At this station, the
22 model better captures the observed AOD with either FINN1 (NMBF= -0.85, $r^2=0.84$) or
23 GFAS1 (NMBF= -1.02, $r^2=0.81$) emissions than with GFED3 emissions (NMBF= -1.58,
24 $r^2=0.29$).

25 The improved representation of small fire emissions in FINN1 and GFAS1 may also explain
26 the improved agreement between modelled and observed PM_{2.5} (Sect. 4.1.1) and AOD (Sect.
27 4.1.2) towards the end of the burning season (~October-November) in Amazonia. Kaiser et al.
28 (2012) report that GFAS1 exhibits slightly longer fire seasons in South America than GFED3.
29 Fires occurring at the tail end of the biomass burning season may be smaller in size and thus
30 better captured by using an active-fire based emission inventory (GFAS1 and FINN1
31 emissions). While at the peak of the burning season in Amazonia, when fires are potentially

1 larger, the comparisons in Sects. 4.1.1 and 4.1.2 suggest that GFED3 emissions capture the
2 observations better than FINN1 or GFAS1.

3 In Indochina, there is improved agreement between simulated and observed AOD with
4 FINN1 emissions ([Fig. 6a](#); NMBF= -0.26 to 0.19, $r^2=0.14-0.98$) relative to both GFED3
5 (NMBF= -0.54 to -0.08, $r^2=0.11-0.84$) and GFAS1 (NMBF= -0.51 to -0.08, $r^2=0.03-0.83$).
6 [Figure 87](#) compares the model with different emissions against observations at the nine
7 AERONET sites in Indochina. FINN1 emissions lead to an improved correlation with
8 observations [at all sites and a reduced root mean square model error at six sites](#) compared to
9 GFED3 and GFAS1. [Figure 98](#) compares the multi-annual average seasonal cycle in AOD at
10 ~~four~~three sites in Thailand. The model with GFED3 and GFAS1 emissions underestimates
11 AOD observed during the dry season (~January – May), whereas the model with FINN1
12 emissions captures the magnitude of dry season AOD reasonably well.

13 AERONET sites in Indochina (located in north and central Thailand and Vietnam) are
14 influenced by local agricultural burning (Li et al., 2013; Lin et al., 2013; Sayer et al., 2014) of
15 sugarcane and rice crop residues (Gadde et al., 2009; Sornpoon et al., 2014). Agricultural fires
16 are typically smaller than other fire types (e.g., deforestation, grassland/savannah and forest),
17 with burned areas of ~0.3 to ~16 ha reported for individual agricultural fires in the US
18 (McCarty et al., 2009) and Africa (Eva and Lambin, 1998). The prevalence of small fires in
19 Indochina may explain why FINN1 emissions result in better prediction of AOD compared to
20 GFED3 in this region.

21 We do not find an improved prediction of AOD with GFAS1 compared to GFED3 in this
22 region, although this would be expected since GFAS1 better captures emissions from small
23 fires than GFED3 (Kaiser et al., 2012). However, the GFAS1 FRP is converted to dry matter
24 burned using GFED3 data (Heil et al., 2010; [Kaiser et al., 2012](#)), which may lead to an
25 underestimation of small fire emissions in some regions. Conversely, FINN1 assumes a
26 relatively large burned area of 1 km² (100 ha) for individual agricultural fires and therefore
27 may overestimate emission fluxes in agricultural fire regions. However, since many small
28 fires may be undetected as fire hotspots by MODIS (due to factors such as the small size of
29 the fires, orbital gaps, persistent cloud cover and the timing of satellite overpass i.e. the
30 potential to miss fires events), by oversizing the area of individual burns, the FINN1
31 emissions may compensate for missing fire detections in this region (B. Yokelson, personal
32 communication, 2014).

1 **4.3 Scaling biomass burning emissions**

2 Previous model simulations, summarised in Table 2, underestimate AOD in regions impacted
3 by biomass burning. To improve simulation of AOD, these studies have scaled particulate
4 emissions from biomass burning (or aerosol concentrations) by a factor of 1.02 to 6. We have
5 found that our model with three different fire emission datasets also underestimates both
6 PM_{2.5} and AOD across tropical regions (although to a lesser extent in Southeast Asia). In this
7 section we explore the impact of scaling biomass burning emissions on simulated AOD and
8 PM_{2.5} concentrations. We performed two sensitivity simulations with each emission
9 inventory where we perturbed the biomass burning emission fluxes of BC and POM upwards
10 by factors of 1.5 and 3.4 (as recommended for GFED3 and GFAS1 by Kaiser et al. (2012)).

11 | Figures [3b](#) and [3c](#) show the NMBF and correlation between simulated and observed multi-
12 annual monthly mean PM_{2.5} concentrations for the two simulations with scaled biomass
13 burning emissions. The outcome of scaling the emissions by a factor of 1.5 depends on the
14 site location. At the sites strongly impacted by biomass burning, the model bias in PM_{2.5} is
15 reduced (FINNx1.5: -0.16 to 0.08; GFEDx1.5: -0.67 to -0.15; GFASx1.5: -0.89 to -0.22) with
16 little change in the correlation. At the preserved forest site near Manaus, the positive model
17 bias is increased (FINNx1.5: 1.33; GFASx1.5: 0.69; GFEDx1.5: 0.66). The outcome of
18 scaling the emissions by a factor of 3.4 depends on both the site location and the emission
19 dataset. The model bias is increased at all sites with FINN1 emissions (0.63-2.72), with mixed
20 results for GFED3 (-0.39 to 1.18) and GFAS1 (-0.16 to 1.25) emissions. Any scaling of the
21 emissions leads to an overestimation of PM_{2.5} at Manaus with all three emission datasets.

22 In summary, a scaling factor of 1.5 applied to the FINN1 emissions is adequate for the model
23 to capture surface PM_{2.5} concentrations observed in regions of high fire activity in the
24 Amazon region. In contrast, the GFAS1 emissions require a larger scaling factor (closer to
25 3.4) for the model to capture surface PM_{2.5} observed at these sites.

26 The results of scaling the GFED3 emissions are more complex. Scaling GFED3 emissions by
27 a factor of 1.5, the model bias becomes relatively small at Alta Floresta (-0.36) and Porto
28 Velho (-0.15) but remains large and negative at Santarem (-0.67). Scaling the emissions by a
29 factor of 3.4 reduces the model bias at Santarem (-0.39), but leads to an overestimation of
30 PM_{2.5} at the other three sites (0.33-1.18). At Santarem, scaling GFED3 emissions by a factor
31 3.4 only marginally improves agreement with the observations; the correlation remains below
32 0.5 and model bias remains negative (despite a positive model bias at the other sites). This is

1 because GFED3 emission fluxes in the peak biomass burning season months in the region of
2 Santarem (November and December) are very low or non-existent, likely due to an omission
3 of small fires (Sect. 4.2), thus there are very few emissions to scale. This result suggests that
4 even by scaling GFED3 emissions by a large factor it is still possible to underestimate PM
5 from fires in regions influenced by emissions from small fires.

6 Figures [6a and 6b](#) show the NMBF and correlation between simulated and observed multi-
7 annual monthly mean AOD with scaled biomass burning emissions. ~~In general, in order to~~
8 ~~match observed AOD, the model requires higher scaling factors to be applied than for surface~~
9 ~~PM2.5.~~ For the model with GFAS1 emissions, scaling by a factor of 3.4 reduces the model
10 bias at all but one site [in Indochina, Africa and South America](#) (relative to the simulations
11 without scaling or with a scaling factor of 1.5), resulting in the best overall match to observed
12 AOD in these regions. [In Equatorial Asia the scaling required to capture observed AOD](#)
13 [depends on the site location \(two sites require no scaling and two sites require a scaling factor](#)
14 [of either 1.5 or 3.4\).](#)

15 [For GFED3 emissions, scaling by a factor of 3.4 results in the best overall match to observed](#)
16 [AOD in Africa and Indochina, but leads to an increased model bias at half the sites in South](#)
17 [America.](#) However, even with a scaling factor of 3.4, the model with GFED3 emissions
18 continues to underestimate observed AOD in north Brazil (Belterra; NMBF= -0.94),
19 indicating that a large scaling factor does not fully compensate for the likely omission of
20 small fire emissions in this inventory (Sect. 4.2). [The overall result of scaling GFED3](#)
21 [emissions in Equatorial Asia is the same for GFAS1 emissions.](#)

22 Scaling FINN1 emissions by a factor of 3.4 improves the agreement with observed AOD in
23 Africa (at all sites), [but generally leads to overestimation and increased model bias at sites in](#)
24 [South America and](#) Southeast Asia. Scaling FINN1 emissions by a factor of 1.5 is adequate to
25 capture observed AOD at the majority of sites in [South America \(mean NMBF= -0.16\), with](#)
26 [no scaling required for the majority of sites in](#) Indochina (mean NMBF= 0.02) and Equatorial
27 Asia (mean NMBF= 0.02).

28 We note that even with a scaling factor of 3.4 applied to the biomass burning emissions, the
29 model underestimates observed AOD at the African AERONET sites with all three fire
30 emission inventories (mean NMBF= -0.31). This may indicate that a larger scaling factor is
31 required to capture observations in this region. However, using a too high scaling factor is
32 likely to compensate for model error e.g. too efficient removal of aerosol or underestimation

1 of dust emissions, and therefore overestimate the contribution of biomass burning to AOD.
2 The potential for compensation errors with emission scaling is relevant for all three regions.
3 For example, in South America the model bias in AOD in the wet season (~December to
4 May) is increased at four or more sites when the FINN1, GFED3, and GFAS1 emissions are
5 scaled by a factor of 3.4, which may be an indication of compensation errors. Compensation
6 errors are also likely to be occurring when emissions are scaled by a factor of 3.4 at sites in
7 urban locations (see Table S1 for location classifications), where a global model is unable to
8 capture sub-grid-scale urban emissions.

9 **5. Conclusions**

10 We have used the GLOMAP global aerosol model evaluated against surface PM2.5
11 observations and AERONET AOD to better understand the impacts of fires on tropical
12 aerosol. We compared three different satellite-derived fire emission datasets (GFED3, GFAS1
13 and FINN1). Total pan-tropical particulate emission (BC+OC) varied by less than 30%
14 between the different emission datasets. Regional differences were much larger (often
15 exceeding 100%) leading to important differences in aerosol concentrations simulated by the
16 global model.

17 We found that GLOMAP underestimated both PM2.5 and AOD in regions strongly impacted
18 by biomass burning, with all emission datasets. The largest underestimation of AOD occurred
19 across Africa, which may be partly due to a large contribution of dust. The smallest
20 underestimation of AOD occurred over Equatorial Asia, where the contribution of fire
21 emissions to simulated AOD was also smallest. Overall, the smallest bias between model and
22 both PM2.5 and AOD observations was found using FINN1 emissions. The model with
23 FINN1 emissions also best simulated the seasonal variability of AOD over Indochina,
24 potentially because of the dominance of smaller fires in this region that are better captured by
25 the FINN1 dataset.

26 In South America where we have coincident surface PM2.5 and AOD observations,
27 underestimation of AOD is greater than underestimation of surface PM2.5 in some locations.
28 We suggest this discrepancy could be caused by errors in i) vertical profile of aerosol, ii)
29 aerosol optical properties, size distribution and hygroscopic growth, or iii) model spatial
30 resolution. In particular, we find that simulated AOD is very sensitive to the calculation of
31 hygroscopic growth, with the magnitude of AOD ranging by a factor of ~1.7 between upper
32 and lower estimates. Detailed vertical profiles of aerosol properties over regions impacted by

1 fires are required to understand and resolve these issues. We caution against using AOD to
2 scale emissions before these issues are fully understood.

3 Particulate emissions from biomass burning are very uncertain with previous studies
4 underestimating AOD in regions impacted by fires and scaling particulate emissions by up to
5 a factor of 6 to help match observations (see Table 2). For each emission dataset we ran two
6 additional simulations where we scaled emissions up by factors of 1.5 and 3.4. We find that
7 the scaling that results in the best agreement with observations is regionally variable and
8 depends on the emission dataset used. With FINN1 emissions, PM2.5 concentrations and
9 AOD in South America are well simulated when emissions are increased by 50%, whereas
10 AOD in Africa is more consistent with a factor 3.4 scaling. In Southeast Asia, observed AOD
11 is well simulated without any scaling applied; scaling FINN1 emissions by 50% generally
12 leads to overestimation in this region. With GFAS1 emissions, PM2.5 concentrations in South
13 America and AOD in South America, Africa and Indochina are best simulated when
14 emissions are scaled by a factor 3.4. With GFED3 emissions, observations of PM2.5 in north
15 Brazil and AOD in Africa, Indochina and some regions of South America are also better
16 simulated with a factor 3.4 scaling; for PM2.5 concentrations and AOD observed in active
17 deforestation regions of South America, a 50% scaling is sufficient. In Equatorial Asia, the
18 results of scaling both GFAS1 and GFED3 emissions are mixed and depend on site location;
19 overall observed AOD is captured best either without scaling or with a scaling factor of 1.5.

20

21 A factor 1.5 scaling is within the uncertainty of emission datasets and is substantially smaller
22 than the emission scaling applied by many other studies (see Table 2). We also note that a
23 factor 1.5 scaling is within the uncertainty of assumed OM to OC ratios; we assume an
24 OM:OC ratio of 1.4 which is at the low end of other studies (Tsigaridis et al., 2014). Scaling
25 fire emissions by a factor of 3.4 to match AOD is likely to partly compensate for an
26 underestimation of aerosol from other sources e.g. dust and/or urban emissions and may also
27 compensate for errors in modelling of the aerosol distribution or calculation of AOD
28 (discussed above). In addition to these factors, we have treated biomass burning emissions as
29 primary and non-volatile. Formation of semi-volatile SOA in biomass burning plumes may be
30 important (Konovalov et al., 2015; Shrivastava et al., 2015) and needs to be explored in future
31 work.

1 Problems with the detection of small fires are an acknowledged issue for GFED3, which
2 relies on detections of area burned to derive emissions (Randerson et al., 2012). Over regions
3 that are likely dominated by small fires the model with GFED3 emissions substantially
4 underestimates both PM_{2.5} (north Brazil) and AOD (north Brazil and Thailand). The model
5 with GFAS1 and FINN1 emissions better simulates aerosol in these regions providing
6 independent evidence that these datasets better represent emissions from small fires. We note
7 that the most recent version of GFED emissions (GFED4) includes an estimate of emissions
8 from small fires (Giglio et al., 2013). Future work should evaluate these emissions against
9 aerosol observations to assess the representation of small fire emissions in the specific regions
10 highlighted here.

11

12 **Acknowledgements**

13 This research was supported by funding from the Natural Environment Research Council for
14 the South American Biomass Burning Analysis (SAMBBA) project (number NE/J009822/1).
15 The authors gratefully acknowledge the principal investigators (listed in Table S1) and their
16 staff responsible for establishing and maintaining the 27 AERONET stations used in this
17 study and providing quality-assured data.

18

19 **References**

20 Akagi, S. K., Yokelson, R. J., Wiedinmyer, C., Alvarado, M. J., Reid, J. S., Karl, T., Crouse,
21 J. D., and Wennberg, P. O.: Emission factors for open and domestic biomass burning for use
22 in atmospheric models, *Atmos. Chem. Phys.*, 11, 4039–4072, doi:10.5194/acp-11-4039-2011,
23 2011.

24 Al-Saadi, J., Soja, A., Pierce, R. B., Szykman, J., Wiedinmyer, C., Emmons, L., Kondragunta,
25 S., Zhang, X., Kittaka, C., Schaack, T., and Bowman, K.: Evaluation of near-real-time
26 biomass burning emissions estimates constrained by satellite fire data, *J. Appl. Remote Sens.*,
27 2, 021504, doi:10.1117/1.2948785, 2008.

28 [Andela, N., Kaiser, J. W., Heil, A., van Leeuwen, T. T., van der Werf, G. R., Wooster, M. J.,](#)
29 [Remy, S. and Schultz, M. G.: Assessment of the Global Fire Assimilation System \(GFASv1\),](#)
30 [MACC-II Project Report, 2013.](#)

31 Andreae, M. O. and Merlet, P.: Emission of trace gases and aerosols from biomass burning,
32 *Global Biogeochem. Cy.*, 15, 955–966, 2001.

33 [Andreae, M. O., Rosenfeld, D., Artaxo, P., Costa, A. A., Frank, G. P., Longo, K. M., and](#)
34 [Silva-Dias, M. A. F.: Smoking rain clouds over the Amazon, *Science*, 303, 1337–1342,](#)
35 [doi:10.1126/science.1092779, 2004.](#)

1 Arnold, S. R., Chipperfield, M. P., and Blitz, M. A.: A three dimensional model study of the
2 effect of new temperature dependent quantum yields for acetone photolysis, *J. Geophys. Res.*,
3 110, D22305, doi:10.1029/2005JD005998, 2005.

4 [Artaxo, P., Rizzo, L. V., Brito, J. F., Barbosa, H. M. J., Arana, A., Sena, E. T., Cirino, G. G.,
5 Bastos, W., Martin, S. T., and Andreae, M. O.: Atmospheric aerosols in Amazonia and land
6 use change: From natural biogenic to biomass burning conditions, *Faraday Discuss.* 165, 203–
7 235, 2013.](#)

8 Bauer, S. E., Menon, S., Koch, D., Bond, T. C., and Tsigaridis, K.: A global modeling study
9 on carbonaceous aerosol microphysical characteristics and radiative effects, *Atmos. Chem.*
10 *Phys.*, 10, 7439–7456, doi:10.5194/acp-10-7439-2010, 2010.

11 [Bian, H., Chin, M., Rodriguez, J. M., Yu, H., Penner, J. E., and Strahan, S.: Sensitivity of
12 aerosol optical thickness and aerosol direct radiative effect to relative humidity, *Atmos.*
13 *Chem. Phys.*, 9, 2375-2386, doi:10.5194/acp-9-2375-2009, 2009.](#)

14 [Bistinas, I., Harrison, S. P., Prentice, I. C., and Pereira, J. M. C.: Causal relationships versus
15 emergent patterns in the global controls of fire frequency, *Biogeosciences*, 11, 5087-5101,
16 doi:10.5194/bg-11-5087-2014, 2014.](#)

17 [Bellouin, N., Rae, J., Jones, A. Johnson, C., Haywood, J. and Boucher, O.: Aerosol forcing in
18 the Climate Model Intercomparison Project \(CMIP5\) simulations by HadGEM2-ES and the
19 role of ammonium nitrate, *J. Geophys. Res.*, 116, D20206, doi:10.1029/2011JD016074, 2011.](#)

20 Browse, J., Carslaw, K. S., Arnold, S. R., Pringle, K., and Boucher, O.: The scavenging
21 processes controlling the seasonal cycle in Arctic sulphate and black carbon aerosol, *Atmos.*
22 *Chem. Phys.*, 12, 6775-6798, doi:10.5194/acp-12-6775-2012, 2012.

23 Carlson, K. M., Curran, L. M., Ratnasari, D., Pittman, A. M., Soares-Filho, B. S., Asner, G.
24 P., Trigg, S. N., Gaveau, D. A., Lawrence, D. and Rodrigues, H. O.: Committed carbon
25 emissions, deforestation, and community land conversion from oil plam plantation expansion
26 in West Kalimantan, Indonesia. *Proc. Natl. Acad. Sci USA*, 109 (19), 7559-7564, 2012.

27 Carslaw, K. S., Lee, L. A., Reddington, C. L., Pringle, K. J., Rap, A., Forster, P. M., Mann, G.
28 W., Spracklen, D. V., Woodhouse, M. T., Regayre, J. R., and Pierce, L. A.: Large
29 contribution of natural aerosols to uncertainty in indirect forcing, *Nature*, 503.7474, 67–71,
30 2013.

31 [Cesnulyte, V., Lindfors, A. V., Pitkänen, M. R. A., Lehtinen, K. E. J., Morcrette, J.-J., and
32 Arola, A.: Comparing ECMWF AOD with AERONET observations at visible and UV
33 wavelengths, *Atmos. Chem. Phys.*, 14, 593-608, doi:10.5194/acp-14-593-2014, 2014.](#)

34 [Chen, X. and Yu, J.: Measurement of organic mass to organic carbon ratio in ambient aerosol
35 samples using a gravimetric technique in combination with chemical analysis, *Atmos.*
36 *Environ.*, 41, 8857–8864, 2007.](#)

37 [Chew, B., Campbell, J., Reid, J., Giles, D., Welton, E., Salinas, S., and Liew, S.: Tropical
38 cirrus cloud contamination in sun photometer data, *Atmos. Environ.*, 45 \(37\), 6724-6731,
39 2011.](#)

40 [Chin, M., Diehl, T., Dubovik, O., Eck, T. F., Holben, B. N., Sinyuk, A., and Streets, D. G.:
41 Light absorption by pollution, dust, and biomass burning aerosols: a global model study and
42 evaluation with AERONET measurements, *Ann. Geophys.*, 27, 3439-3464,
43 doi:10.5194/angeo-27-3439-2009, 2009.](#)

- 1 Chipperfield, M. P.: New version of the TOMCAT/SLIMCAT offline chemical transport
2 model: Intercomparison of stratospheric tracer experiments, *Q. J. Roy. Meteor. Soc.*, 132,
3 1179–1203, 2006.
- 4 Cochrane, M. A. and Laurance, W. F.: Fire as a large-scale edge effect in Amazonian forests,
5 *J. Trop. Ecol.*, 18, 311–325, 2002.
- 6 Cooke, W. F. and Wilson, J. J. N.: A global black carbon model, *J. Geophys. Res.*, 101,
7 19,395–19,409, 1996.
- 8 Cox, P. M., Harris, P. P., Huntingford, C., Betts, R. A., Collins, M., Jones, C. D., Jupp, T. E.,
9 Marengo, J. A., and Nobre, C. A.: Increasing risk of Amazonian drought due to decreasing
10 aerosol pollution, *Nature*, 453, 212–216, doi:10.1038/nature06960, 2008.
- 11 Crutzen, P. J. and Andreae, M. O.: Biomass burning in the tropics: Impact on atmospheric
12 chemistry and biogeochemical cycles, *Science*, 250, 1669–1678, 1990.
- 13 Daskalakis, N., Myriokefalitakis, S., and Kanakidou, M.: Sensitivity of tropospheric loads and
14 lifetimes of short lived pollutants to fire emissions, *Atmos. Chem. Phys.*, 15, 3543–3563,
15 doi:10.5194/acp-15-3543-2015, 2015.
- 16 [DeMott, P. J., Petters, M. D., Prenni, A. J., Carrico, C. M., Kreidenweis, S. M., Collett Jr., J.
17 L., and Moosmüller, H.: Ice nucleation behavior of biomass combustion particles at cirrus
18 temperatures, *J. Geophys. Res.*, 114, D16205, doi:10.1029/2009JD012036, 2009.](#)
- 19 Dentener, F., Kinne, S., Bond, T., Boucher, O., Cofala, J., Generoso, S., Ginoux, P., Gong, S.,
20 Hoelzemann, J.J., Ito, A., Marelli, L., Penner, J.E., Putaud, J.-P., Textor, C., Schulz, M., van
21 der Werf, G.R., and Wilson, J.: Emissions of primary aerosol and precursor gases in the years
22 2000 and 1750 prescribed data-sets for AeroCom, *Atmos. Chem. Phys.*, 6, 4321–4344,
23 doi:10.5194/acp-6-4321-2006, 2006.
- 24 Doughty, C. E., Flanner, M. G., and Goulden, M. L.: Effect of smoke on subcanopy shaded
25 light, canopy temperature, and carbon dioxide uptake in an Amazon rainforest, *Global
26 Biogeochem. Cycles*, 24, GB3015, doi:10.1029/2009GB003670, 2010.
- 27 Emmanuel, S.C.: Impact to lung health of haze from forest fires: The Singapore experience,
28 *Respirology*, 5, 175–182, 2000.
- 29 Eva, H. and Lambin, E. F.: Remote sensing of biomass burning in tropical regions: Sampling
30 issues and multisensor approach, *Remote Sens. Environ.*, 64(3), 292–315, doi:10.1016/S0034-
31 4257(98)00006-6, 1998.
- 32 Feingold, G., Jiang, H., and Harrington, J. Y.: On smoke suppression of clouds in Amazonia,
33 *Geophys. Res. Lett.*, 32, L02804, doi:10.1029/2004GL021369, 2005.
- 34 Field, R. D., van der Werf, G. R., and Shen, S. S. P.: Human amplification of drought-induced
35 biomass burning in Indonesia since 1960, *Natl. Geosci.*, 2, 185–188, doi:10.1038/NGEO443,
36 2009.
- 37 Frankenberg, E., McKee, D. and Thomas, D.: Health consequences of forest fires in
38 Indonesia, *Demography*, 42, 109–129, 2005.
- 39 Gadde, B., Bonnet, S., Menke, C. and Garivait, S.: Air pollutant emissions from rice straw
40 open field burning in India, Thailand and the Philippines, *Environ. Pollut.*, 157, 1554–1558,
41 <http://dx.doi.org/10.1016/j.envpol.2009.01.004>, 2009.
- 42 Giglio, L.: MODIS Collection 4 Active Fire Product User's Guide Version 2.3, Science
43 Systems and Applications, Inc, 2005.

1 Giglio, L., Descloitres, J., Justice, C. O., Kaufman, Y. J.: An enhanced contextual fire
2 detection algorithm for MODIS. *Remote Sens. Environ.*, 87, 273–282, 2003.

3 Giglio, L., Randerson, J. T., van der Werf, G. R., Kasibhatla, P. S., Collatz, G. J., Morton, D.
4 C., and DeFries, R. S.: Assessing variability and long-term trends in burned area by merging
5 multiple satellite fire products, *Biogeosciences*, 7, 1171–1186, doi:10.5194/bg-7-1171-2010,
6 2010.

7 Giglio, L., Randerson, J. T., and van der Werf, G. R.: Analysis of daily, monthly, and annual
8 burned area using the fourth-generation global fire emissions database (GFED4) *J. Geophys.*
9 *Res. Biogeosci.*, 118, 317–328, doi:10.1002/jgrg.20042, 2013.

10 Golding, N. and Betts, R.: Fire risk in Amazonia due to climate change in the HadCM3
11 climate model: Potential interactions with deforestation, *Global Biogeochem. Cycles*, 22,
12 GB4007, doi:10.1029/2007GB003166, 2008.

13 Gonçalves, W. A., Machado, L. A. T., and Kirstetter, P.-E.: Influence of biomass aerosol on
14 precipitation over the Central Amazon: an observational study, *Atmos. Chem. Phys.*, 15,
15 6789–6800, doi:10.5194/acp-15-6789-2015, 2015.

16 Guenther, A., Hewitt, C. N., Erickson, D., Fall, R., Geron, C., Graedel, T., Harley, P.,
17 Klinger, L., Lerdau, M., McKay, W. A., Pierce, T., Scholes, B., Steinbrecher, R.,
18 Tallamraju, R., Taylor, J., and Zimmerman, P.: A global model of natural volatile organic
19 compound emissions, *J. Geophys. Res.*, 100(D5), 8873–8892, 1995.

20 [Grainger, R. G., Lucas, J., Thomas, G. E., and Ewen, G. B. L.: Calculation of Mie](#)
21 [Derivatives, *Appl. Opt.*, 43, 5386, doi:10.1364/AO.43.005386, 2004.](#)

22 [Granier, C., Bessagnet, B., Bond, T., D'Angiola, A., Denier van der Gon, H., Frost, G. J.,](#)
23 [Heil, A., Kaiser, J. W., Kinne, S., Klimont, Z., Kloster, S., Lamarque, J.-F., Liousse, C.,](#)
24 [Masui, T., Meleux, F., Mieville, A., Ohara, T., Raut, J.-C., Riahi, K., Schultz, M. G., Smith,](#)
25 [S. J., Thompson, A., Aardenne, J., van der Werf, G. R., Vuuren, D. P.: Evolution of](#)
26 [anthropogenic and biomass burning emissions of air pollutants at global and regional scales](#)
27 [during the 1980–2010 period, *Clim. Change*, 109, 163–190, 2011.](#)

28 [Haywood, J. M., Osborne, S. R., Francis, P. N., Keil, A., Formenti, P., Andreae, M. O., and](#)
29 [Kaye, P. H.: The mean physical and optical properties of regional haze dominated by biomass](#)
30 [burning aerosol measured from the C-130 aircraft during SAFARI 2000, *J. Geophys. Res.*,](#)
31 [108\(D13\), 8473, doi:10.1029/2002JD002226, 2003.](#)

32 [Heald, C. L., and Spracklen, D. V.: Land use change impacts on air quality and climate,](#)
33 [*Chem. Rev.*, 115 \(10\), 4476–4496, doi: 10.1021/cr500446g, 2015.](#)

34 [Heil, A., Kaiser, J. W., van der Werf, G. R., Wooster, M. J., Schultz, M. G., and Dernier van](#)
35 [der Gon, H.: Assessment of the Real-Time Fire Emissions \(GFASv0\) by MACC, Tech.](#)
36 [Memo. 628, ECMWF, Reading, UK, 2010.](#)

37 [Huang, K., Fu, J. S., Hsu, N. C., Gao, Y., Dong, X., Tsay, S.-C., and Lam, Y. F.: Impact](#)
38 [assessment of biomass burning on air quality in Southeast and East Asia during BASE-ASIA,](#)
39 [*Atmos. Environ.*, 78, 291–302, 2013.](#)

40 Holben, B. N., Eck, T. F., Slutsker, I., Tanré, D., Buis, J. P., Setzer, A., Vermote, E., Reagan,
41 J. A., Kaufman, Y. J., Nakajima, T., Lavenue, F., Jankowiak, I., and Smirnov, A.:
42 AERONET—A Federated Instrument Network and Data Archive for Aerosol
43 Characterization, *Remote Sens. Environ.*, 66, 1, 1–16, <http://dx.doi.org/10.1016/S0034->
44 [4257\(98\)00031-5](http://dx.doi.org/10.1016/S0034-4257(98)00031-5), 1998.

- 1 Hoelzemann, J. J., Schultz, M. G., Brasseur, G. P., Granier, C., and Simon, M.: Global
2 Wildland Fire Emission Model (GWEM): evaluating the use of global area burnt satellite
3 data, *J. Geophys. Res.*, 109, D14S04, doi:10.1029/2003JD003666, 2004.
- 4 Ichoku, C. and Ellison, L.: Global top-down smoke-aerosol emissions estimation using
5 satellite fire radiative power measurements, *Atmos. Chem. Phys.*, 14, 6643-6667,
6 doi:10.5194/acp-14-6643-2014, 2014.
- 7 Ito, A. and Penner, J. E.: Global estimates of biomass burning emissions based on satellite
8 imagery for the year 2000, *J. Geophys. Res.*, 109, D14S05, doi:10.1029/2003JD004423,
9 2004.
- 10 Ito, A. and J. E. Penner: Estimates of CO emissions from open biomass burning in southern
11 Africa for the year 2000, *J. Geophys. Res.*, 110, D19306, doi:10.1029/2004JD005347, 2005.
- 12 Jacobson, M. Z., Effects of biomass burning on climate, accounting for heat and moisture
13 fluxes, black and brown carbon, and cloud absorption effects, *J. Geophys. Res. Atmos.*, 119,
14 8980–9002, doi:10.1002/2014JD021861, 2014.
- 15 Jacobson, L.d.S.V., Hacon, S.d.S., Castro, H.A.d., Ignotti, E., Artaxo, P., Saldiva, P.H.N.,
16 Leon, A.C.M. P.d.: Acute effects of particulate matter and black carbon from seasonal fires on
17 peak expiratory flow of schoolchildren in the Brazilian Amazon, *Plos One*, 9(8): e104177,
18 doi:10.1371/journal.pone.0104177, 2014.
- 19 [Jathar, S. H., Gordon, T. D., Hennigan, C. J., Pye, H. O. T., Pouliot, G., Adams, P. J.,](#)
20 [Donahue, N. M., Robinson, A. L.: Unspeciated organic emissions from combustion sources](#)
21 [and their influence on the secondary organic aerosol budget in the United States. *Proc. Natl.*](#)
22 [*Acad. Sci USA*, 111\(29\), 10473-10478, 2014.](#)
- 23 Johnson, B. T., Heese, B., McFarlane, S. A., Chazette, P., Jones, A., and Bellouin, N.:
24 Vertical distribution and radiative effects of mineral dust and biomass burning aerosol over
25 West Africa during DABEX, *J. Geophys. Res.*, 113, D00C12, doi:10.1029/2008JD009848,
26 2008.
- 27 Johnston, F. H., Henderson, S. B., Chen, Y., Randerson, J. T., Marlier, M., Defries, R. S.,
28 Kinney, P., Bowman, D. M. and Brauer, M.: Estimated global mortality attributable to smoke
29 from landscape fires, *Environ. Health Perspect.*, 120, 695-701, 2012.
- 30 Justice, C. O., Giglio, L., Korontzi, S., Owens, J., Morisette, J. T., Roy, D., Descloitres, J.,
31 Alleaume, S., Petitcolin, F., and Kaufman, Y.: The MODIS fire products, *RSE*, 83, 244–262,
32 2002.
- 33 Kaiser, J. W., Heil, A., Andreae, M. O., Benedetti, A., Chubarova, N., Jones, L., Morcrette,
34 J.-J., Razinger, M., Schultz, M. G., Suttie, M., and van der Werf, G. R.: Biomass burning
35 emissions estimated with a global fire assimilation system based on observations of fire
36 radiative power, *Biogeosciences*, 9, 527-554, doi:10.5194/bg-9-527-2012, 2012.
- 37 [Kolusu, S. R., Marsham, J. H., Mulcahy, J., Johnson, B., Dunning, C., Bush, M., and](#)
38 [Spracklen, D. V.: Impacts of Amazonia biomass burning aerosols assessed from short-range](#)
39 [weather forecasts, *Atmos. Chem. Phys.*, 15, 12251-12266, doi:10.5194/acp-15-12251-2015,](#)
40 [~~2015. Kolusu, S. R., Marsham, J. H., Muleahy, J., Johnson, B., Dunning, C., Bush, M., and~~](#)
41 [~~Spracklen, D. V.: Impacts of Amazonia biomass burning aerosols assessed from short-range~~](#)
42 [~~weather forecasts, *Atmos. Chem. Phys. Discuss.*, 15, 18883-18919, doi:10.5194/acpd-15-~~](#)
43 [~~18883-2015, 2015.~~](#)
- 44 [Konovalov, I. B., Berezin, E. V., Ciais, P., Broquet, G., Beekmann, M., Hadji-Lazaro, J.,](#)
45 [Clerbaux, C., Andreae, M. O., Kaiser, J. W., and Schulze, E.-D.: Constraining CO2 emissions](#)

1 [from open biomass burning by satellite observations of co-emitted species: a method and its](#)
2 [application to wildfires in Siberia, *Atmos. Chem. Phys.*, 14, 10383-10410, doi:10.5194/acp-](#)
3 [14-10383-2014, 2014.](#)

4 [Konovalov, I. B., Beekmann, M., Berezin, E. V., Petetin, H., Mielonen, T., Kuznetsova, I. N.,](#)
5 [and Andreae, M. O.: The role of semi-volatile organic compounds in the mesoscale evolution](#)
6 [of biomass burning aerosol: a modeling case study of the 2010 mega-fire event in Russia,](#)
7 [Atmos. Chem. Phys., 15, 13269-13297, doi:10.5194/acp-15-13269-2015, 2015.](#)

8 Lamarque, J.-F., Bond, T. C., Eyring, V., Granier, C., Heil, A., Klimont, Z., Lee, D., Liousse,
9 D., Mieville, A., Owen, B., Schultz, M. G., Shindell, D., Smith, S. J., Stehfest, E., Van
10 Aardenne, J., Cooper, O. R., Kainuma, M., Mahowald, N., McConnell, J. R., Naik, V., Riahi,
11 K., and van Vuuren, D. P.: Historical (1850-2000) gridded anthropogenic and biomass
12 burning emissions of ozone and aerosol precursors: methodology and application. *Atmos.*
13 *Chem. Phys.*, 10, 7017–7039, doi:10.5194/acp-10-7017-2010, 2010.

14 Lee, L. A., Pringle, K. J., Reddington, C. L., Mann, G. W., Stier, P., Spracklen, D. V., Pierce,
15 J. R., and Carslaw, K. S.: The magnitude and causes of uncertainty in global model
16 simulations of cloud condensation nuclei, *Atmos. Chem. Phys.*, 13, 8879-8914,
17 doi:10.5194/acp-13-8879-2013, 2013.

18 Li, C., Tsay, S.-C., Hsu, N. C., Kim, J. Y., Howell, S. G., Huebert, B. J., Ji, Q., Jeong, M.-J.,
19 Wang, S.-H., Hansell, R. A., and Bell, S. W.: Characteristics and composition of atmospheric
20 aerosols in Phimai, central Thailand during BASE-ASIA, *Atmos. Environ.*, 78, 60–71, 2013.

21 Lin, N.-H., Tsay, S.-C., Maring, H. B., Yen, M.-C., Sheu, G.-R., Wang, S.-H., Chi, K. H.,
22 Chuang, M.-T., Ou-Yang, C.-F., Fu, J. S., Reid, J. S., Lee, C.-T., Wang, L.-C., Wang, J.-L.,
23 Hsu, C. N., Sayer, A. M., Holben, B. N., Chu, Y.-C., Nguyen, X. A., Sopajaree, K., Chen, S.-
24 J., Cheng, M.-T., Tsuang, B.-J., Tsai, C.-J., Peng, C.-M., Schnell, R. C., Conway, T., Chang,
25 C.-T., Lin, K.-S., Tsai, Y. I., Lee, W.-J., Chang, S.-C., Liu, J.-J., Chiang, W.-L., Huang, S.-J.,
26 Lin, T.-H., and Liu, G.-R.: An overview of regional experiments on biomass burning aerosols
27 and related pollutants in Southeast Asia: From BASE-ASIA and the Dongsha Experiment to
28 7-SEAS, *Atmos. Environ.*, 78, 1–19, 2013.

29 Liousse, C., Penner, J. E., Chuang, C., Walton, J. J., Eddleman, H., and Cachier, H.: A global
30 three-dimensional model study of carbonaceous aerosols, *J. Geophys. Res.*, 101, 19411-
31 19432, 1996.

32 Liousse, C., Guillaume, B., Grégoire, J. M., Mallet, M., Galy, C., Pont, V., Akpo, A., Bedou,
33 M., Castéra, P., Dungall, L., Gardrat, E., Granier, C., Konaré, A., Malavelle, F., Mariscal, A.,
34 Mieville, A., Rosset, R., Serça, D., Solmon, F., Tummon, F., Assamoi, E., Yoboué, V., and
35 Van Velthoven, P.: Updated African biomass burning emission inventories in the framework
36 of the AMMA-IDAF program, with an evaluation of combustion aerosols, *Atmos. Chem.*
37 *Phys.*, 10, 9631-9646, doi:10.5194/acp-10-9631-2010, 2010.

38 Mann, G. W., Carslaw, K. S., Spracklen, D. V., Ridley, D. A., Manktelow, P. T.,
39 Chipperfield, M. P., Pickering, S. J., and Johnson, C. E.: Description and evaluation of
40 GLOMAP-mode: a modal global aerosol microphysics model for the UKCA composition-
41 climate model, *Geosci. Model Dev.*, 3, 519-551, doi:10.5194/gmd-3-519-2010, 2010.

42 Mann, G. W., Carslaw, K. S., Reddington, C. L., Pringle, K. J., Schulz, M., Asmi, A.,
43 Spracklen, D. V., Ridley, D. A., Woodhouse, M. T., Lee, L. A., Zhang, K., Ghan, S. J.,
44 Easter, R. C., Liu, X., Stier, P., Lee, Y. H., Adams, P. J., Tost, H., Lelieveld, J., Bauer, S. E.,
45 Tsigaridis, K., van Noije, T. P. C., Strunk, A., Vignati, E., Bellouin, N., Dalvi, M., Johnson,
46 C. E., Bergman, T., Kokkola, H., von Salzen, K., Yu, F., Luo, G., Petzold, A., Heintzenberg,

- 1 J., Clarke, A., Ogren, J. A., Gras, J., Baltensperger, U., Kaminski, U., Jennings, S. G.,
2 O'Dowd, C. D., Harrison, R. M., Beddows, D. C. S., Kulmala, M., Viisanen, Y., Ulevicius,
3 V., Mihalopoulos, N., Zdimal, V., Fiebig, M., Hansson, H.-C., Swietlicki, E., and Henzing, J.
4 S.: Intercomparison and evaluation of global aerosol microphysical properties among
5 AeroCom models of a range of complexity, *Atmos. Chem. Phys.*, 14, 4679-4713,
6 doi:10.5194/acp-14-4679-2014, 2014.
- 7 Marlier, M. E., DeFries, R. S., Voulgarakis, A., Kinney, P. L., Randerson, J. T., Shindell, D.
8 T., Chen, Y. and Faluvegi, G.: El Niño and health risks from landscape fire emissions in
9 southeast Asia, *Nature Clim. Change*, 3, 131-136, doi:10.1038/nclimate1658, 2013.
- 10 Matichuk, R. I., Colarco, P. R., Smith, J. A., and Toon, O. B.: Modeling the transport and
11 optical properties of smoke aerosols from African savanna fires during the Southern African
12 Regional Science Initiative campaign (SAFARI 2000), *J. Geophys. Res.*, 112, D08203,
13 doi:10.1029/2006JD007528, 2007.
- 14 Matichuk, R. I., Colarco, P. R., Smith, J. A. and Toon, O. B.: Modeling the transport and
15 optical properties of smoke plumes from South American biomass burning, *J. Geophys. Res.*,
16 113, D07208, doi:10.1029/2007JD009005, 2008.
- 17 McCarty, J. L., Korontzi, S., Justice, C. O., and Loboda, T.: The spatial and temporal
18 distribution of crop residue burning in the contiguous United States, *Sci. Total Environ.*,
19 407(21), 5701–5712, doi:10.1016/j.scitotenv.2009.07.009, 2009.
- 20 ~~Chin, M., Diehl, T., Dubovik, O., Eck, T. F., Holben, B. N., Sinyuk, A., and Streets, D. G.:
21 Light absorption by pollution, dust, and biomass burning aerosols: a global model study and
22 evaluation with AERONET measurements, *Ann. Geophys.*, 27, 3439-3464,
23 doi:10.5194/angeo-27-3439-2009, 2009.~~
- 24 Malhi, Y., Aragão, L. E. O. C. , Galbraith, D., Huntingford, C., Fisher, R., Zelazowski, P.,
25 Sitch, S., McSweeney, C., and Meir, P.: Exploring the likelihood and mechanism of a climate-
26 change induced dieback of the Amazon rainforest, *P. Natl. Acad. Sci. USA*, 106, 20610–
27 20615, 2009.
- 28 Mu, M., Randerson, J. T., van der Werf, G. R., Giglio, L., Kasibhatla, P., Morton, D., Collatz,
29 G. J., DeFries, R. S., Hyer, E. J., Prins, E. M., Griffith, D. W. T., Wunch, D., Toon, G. C.,
30 Sherlock and V., Wennberg, P. O.: Daily and 3-hourly variability in global fire emissions and
31 consequences for atmospheric model predictions of carbon monoxide, *J. Geophys. Res.*, 116,
32 doi: 10.1029/2011JD016245, 2011.
- 33 Myhre, G., Berntsen, T. K., Haywood, J. M., Sundet, J. K., Holben, B. N., Johnsrud, M., and
34 Stordal, F.: Modeling the solar radiative impact of aerosols from biomass burning during the
35 Southern African Regional Science Initiative (SAFARI-2000) experiment, *J. Geophys. Res.*,
36 108(D13), 8501, doi:10.1029/2002JD002313, 2003.
- 37 Oliveira, P. H. F., Artaxo, P., Pires, C., De Lucca, S., Procopio, A., Holben, B., Schafer, J.,
38 Cardoso, L. F., Wofsy, S. C., and Rocha, H. R.: The effects of biomass burning aerosols and
39 clouds on the CO₂ flux in Amazonia, *Tellus B*, 59, 338–349, 2007.
- 40 Queface, A. J., Piketh, S. J., Eck, T. F., Tsay, S.-C. and Mavume, A.F.: Climatology of
41 aerosol optical properties in Southern Africa, *Atmos. Environ.*, 45, 2910-2921,
42 http://dx.doi.org/10.1016/j.atmosenv.2011.01.056, 2011.
- 43 Pandithurai, G., Pinker, R. T., Dubovik, O., Holben, B. N., and Aro, T.: Remote sensing of
44 aerosol optical characteristics in sub-Sahel, West Africa, *J. Geophys. Res.*, 106, 28347–
45 28356, doi:10.1029/2001JD900234, 2001.

- 1 [Pang, Y., Turpin, B., and Gundel, L.: On the importance of organic oxygen for understanding](#)
2 [organic aerosol particles, *Aerosol Sci. Tech.*, 40, 128–133, 2006.](#)
- 3 [Petters, M. D. and Kreidenweis, S. M.: A single parameter representation of hygroscopic](#)
4 [growth and cloud condensation nucleus activity, *Atmos. Chem. Phys.*, 7, 1961–1971,](#)
5 [doi:10.5194/acp-7-1961-2007, 2007.](#)
- 6 [Petters, M. D., Carrico, C. M., Kreidenweis, S. M., Prenni, A. J., DeMott, P. J., Collett Jr., J.](#)
7 [L., and Moosmüller, H.: Cloud condensation nucleation activity of biomass burning aerosol,](#)
8 [*J. Geophys. Res.*, 114, D22205, doi:10.1029/2009JD012353, 2009.](#)
- 9 [Petrenko, M., Kahn, R., Chin, M., Soja, A., Kucsera, T., and Harshvardhan: The use of](#)
10 [satellite-measured aerosol optical depth to constrain biomass burning emissions source](#)
11 [strength in the global model GOCART, *J. Geophys. Res.*, 117, D18212,](#)
12 [doi:10.1029/2012JD017870, 2012.](#)
- 13 Pierce, J. R. and Adams, P. J.: Uncertainty in global CCN concentrations from uncertain
14 aerosol nucleation and primary emission rates, *Atmos. Chem. Phys.*, 9, 1339–1356,
15 doi:10.5194/acp-9-1339-2009, 2009.
- 16 Pierce, J. R., Chen, K., and Adams, P. J.: Contribution of primary carbonaceous aerosol to
17 cloud condensation nuclei: processes and uncertainties evaluated with a global aerosol
18 microphysics model, *Atmos. Chem. Phys.*, 7, 5447–5466, doi:10.5194/acp-7-5447-2007,
19 2007.
- 20 Ramanathan, V., Crutzen, P. J., Kiehl, J. T., and Rosenfeld, D.: Aerosols, climate, and the
21 hydrological cycle, *Science*, 294, 2119–2124, 2001.
- 22 [Randerson, J. T., Chen, Y., van der Werf, G. R., Rogers, B. M. and Morton, D. C.: Global](#)
23 [burned area and biomass burning emissions from small fires, *J. Geophys. Res.*, 117, G04,012,](#)
24 [doi:10.1029/2012JG002128, 2012.](#)
- 25 Rap, A., Spracklen, D. V., Mercado, L., Reddington, C. L., Haywood, J. M., Ellis, R. J.,
26 Phillips, O. L., Artaxo, P., Bonal, D., Restrepo Coupe, N., and Butt, N.: Fires increase
27 Amazon forest productivity through increases in diffuse radiation, *Geophys. Res. Lett.*, 42,
28 4654–4662, doi:10.1002/2015GL063719, 2015.
- 29 Reddington, C. L., Carslaw, K. S., Spracklen, D. V., Frontoso, M. G., Collins, L., Merikanto,
30 J., Minikin, A., Hamburger, T., Coe, H., Kulmala, M., Aalto, P., Flentje, H., Plass-Dülmer,
31 C., Birmili, W., Wiedensohler, A., Wehner, B., Tuch, T., Sonntag, A., O'Dowd, C. D.,
32 Jennings, S. G., Dupuy, R., Baltensperger, U., Weingartner, E., Hansson, H.-C., Tunved, P.,
33 Laj, P., Sellegri, K., Boulon, J., Putaud, J.-P., Gruening, C., Swietlicki, E., Roldin, P.,
34 Henzing, J. S., Moerman, M., Mihalopoulos, N., Kouvarakis, G., Ždímal, V., Ziková, N.,
35 Marinoni, A., Bonasoni, P., and Duchi, R.: Primary versus secondary contributions to particle
36 number concentrations in the European boundary layer, *Atmos. Chem. Phys.*, 11, 12007-
37 12036, doi:10.5194/acp-11-12007-2011, 2011.
- 38 Reddington, C. L., McMeeking, G., Mann, G. W., Coe, H., Frontoso, M. G., Liu, D., Flynn,
39 M., Spracklen, D. V., and Carslaw, K. S.: The mass and number size distributions of black
40 carbon aerosol over Europe, *Atmos. Chem. Phys.*, 13, 4917-4939, doi:10.5194/acp-13-4917-
41 2013, 2013.
- 42 Reddington, C. L., Yoshioka M., Balasubramanian, R., Ridley, D., Toh, Y. Y., Arnold, S. R.,
43 and Spracklen, D. V.: Contribution of vegetation and peat fires to particulate air pollution in
44 Southeast Asia, *Environ. Res. Lett.*, 9, 094006, 2014.

- 1 [Reddington, C. L., Butt, E. W., Ridley, D. A., Artaxo, P., Morgan, W. T., Coe, H., and](#)
2 [Spracklen, D. V.: Air quality and human health improvements from reductions in](#)
3 [deforestation-related fire in Brazil. *Nat Geosci.*, 8, 768–71, doi:10.1038/ngeo2535, 2015.](#)
- 4 Reid, J. S., Koppmann, R., Eck, T. F., and Eleuterio, D. P.: A review of biomass burning
5 emissions part II: intensive physical properties of biomass burning particles, *Atmos. Chem.*
6 *Phys.*, 5, 799-825, doi:10.5194/acp-5-799-2005, 2005.
- 7 Reid, J. S., Hyer, E. J., Prins, E. M., Westphal, D. L., Zhang, J., Wang, J., Christopher, S. A.,
8 Curtis, C. A., Schmidt, C. C., Eleuterio, D. P., Richardson, K. A., and Hoffman, J. P.: Global
9 monitoring and forecasting of biomass-burning smoke: Description of and lessons from the
10 Fire Locating and Modeling of Burning Emissions (FLAMBE) Program, *IEEE J. Sel. Top.*
11 *Appl.*, 2, 3, 144–162, doi:10.1109/JSTARS.2009.2027443, 2009.
- 12 [Rissler, J., Vestin, A., Swietlicki, E., Fisch, G., Zhou, J., Artaxo, P., and Andreae, M. O.: Size](#)
13 [distribution and hygroscopic properties of aerosol particles from dry-season biomass burning](#)
14 [in Amazonia, *Atmos. Chem. Phys.*, 6, 471-491, doi:10.5194/acp-6-471-2006, 2006.](#)
- 15 Sakaeda, N., R. Wood, and P. J. Rasch: Direct and semidirect aerosol effects of southern
16 African biomass burning aerosol, *J. Geophys. Res.*, 116, D12205,
17 doi:10.1029/2010JD015540, 2011.
- 18 Sayer, A. M., Hsu, N. C., Eck, T. F., Smirnov, A., and Holben, B. N.: AERONET-based
19 models of smoke-dominated aerosol near source regions and transported over oceans, and
20 implications for satellite retrievals of aerosol optical depth, *Atmos. Chem. Phys.*, 14, 11493-
21 11523, doi:10.5194/acp-14-11493-2014, 2014.
- 22 Schmidt, A., Carslaw, K. S., Mann, G. W., Rap, A., Pringle, K. J., Spracklen, D. V., Wilson,
23 M., and Forster, P. M.: Importance of tropospheric volcanic aerosol for indirect radiative
24 forcing of climate, *Atmos. Chem. Phys.*, 12, 7321-7339, doi:10.5194/acp-12-7321-2012,
25 2012.
- 26 Schultz, M. G., Heil, A., Hoelzemann, J. J., Spessa, A., Thonicke, K., Goldammer, J. G.,
27 Held, A. C., Pereira, J. M. C., and van het Bolscher, M.: Global wildland fire emissions from
28 1960 to 2000, *Global Biogeochem. Cy.*, 22, GB2002, doi:10.1029/2007GB003031, 2008.
- 29 Scott, C. E., Rap, A., Spracklen, D. V., Forster, P. M., Carslaw, K. S., Mann, G. W., Pringle,
30 K. J., Kivekäs, N., Kulmala, M., Lihavainen, H., and Tunved, P.: The direct and indirect
31 radiative effects of biogenic secondary organic aerosol, *Atmos. Chem. Phys.*, 14, 447-470,
32 doi:10.5194/acp-14-447-2014, 2014.
- 33 [Seiler, W. and Crutzen, P. J.: Estimates of gross and net fluxes of carbon between the](#)
34 [biosphere and the atmosphere from biomass burning. *Climatic Change*, 2\(3\):207–247, 1980.](#)
- 35 [Shrivastava, M., R. C. Easter, X. Liu, A. Zelenyuk, B. Singh, K. Zhang, P.-L. Ma, D. Chand,](#)
36 [S. Ghan, J. L. Jimenez, Q. Zhang, J. Fast, P. J. Rasch, and P. Tiitta: Global transformation and](#)
37 [fate of SOA: Implications of low-volatility SOA and gas-phase fragmentation reactions. *J.*](#)
38 [Geophys. Res. Atmos., 120,4169–4195. doi: 10.1002/2014JD022563, 2015.](#)
- 39 Sornpoon, W., Bonnet, S., Kasemsap, P., Prasertsak, P., Garivait, S.: Estimation of emissions
40 from sugarcane field burning in Thailand using bottom-up country-specific activity data,
41 *Atmosphere*, 5, 669-685, 2014.
- 42 Spracklen, D. V., Pringle, K. J., Carslaw, K. S., Chipperfield, M. P., and Mann, G. W.: A
43 global off-line model of size-resolved aerosol microphysics: I. Model development and
44 prediction of aerosol properties, *Atmos. Chem. Phys.*, 5, 2227-2252, doi:10.5194/acp-5-2227-
45 2005, 2005a.

- 1 Spracklen, D. V., Pringle, K. J., Carslaw, K. S., Chipperfield, M. P., and Mann, G. W.: A
2 global off-line model of size-resolved aerosol microphysics: II. Identification of key
3 uncertainties, *Atmos. Chem. Phys.*, 5, 3233–3250, doi:10.5194/acp-5-3233-2005, 2005b.
- 4 Spracklen, D. V., Carslaw, K. S., Kulmala, M., Kerminen, V.-M., Mann, G. W., and Sihto,
5 S.-L.: The contribution of boundary layer nucleation events to total particle concentrations
6 on regional and global scales, *Atmos. Chem. Phys.*, 6, 5631–5648, doi:10.5194/acp-6-5631-
7 2006, 2006.
- 8 Spracklen, D. V., Carslaw, K. S., Kulmala, M., Kerminen, V.-M., Sihto, S.-L., Riipinen, I.,
9 Merikanto, J., Mann, G. W., Chipperfield, M. P., Wiedensohler, A., Birmili, W., and
10 Lihavainen, H.: Contribution of particle formation to global cloud condensation nuclei
11 concentrations, *Geophys. Res. Lett.*, 35, L06808, doi:10.1029/2007GL033038, 2008
- 12 Spracklen, D. V., Jimenez, J. L., Carslaw, K. S., Worsnop, D. R., Evans, M. J., Mann, G. W.,
13 Zhang, Q., Canagaratna, M. R., Allan, J., Coe, H., McFiggans, G., Rap, A., and Forster, P.:
14 Aerosol mass spectrometer constraint on the global secondary organic aerosol budget, *Atmos.*
15 *Chem. Phys.*, 11, 12109–12136, doi:10.5194/acp-11-12109-2011, 2011a.
- 16 Spracklen, D. V., Carslaw, K. S., Poschl, U., Rap, A., and Forster, P. M.: Global cloud
17 condensation nuclei influenced by carbonaceous combustion aerosol, *Atmos. Chem. Phys.*,
18 11, 9067–9087, doi:10.5194/acp-11-9067-2011, 2011b.
- 19 [Stokes, R. H. and Robinson, R. A.: Interactions in aqueous nonelectrolyte solutions. I. Solute-](#)
20 [solvent equilibria, *J. Phys. Chem.*, 70, 2126–2130, 1966.](#)
- 21 Swap, R., Garstang, M., Macko, S. A., Tyson, P. D., Maenhaut, W., Artaxo, P., Källberg, P.,
22 and Talbot, R.: The long-range transport of southern African aerosols to the tropical South
23 Atlantic, *J. Geophys. Res.*, 101(D19), 23777–23791, doi:10.1029/95JD01049, 1996.
- 24 Tosca, M. G., Randerson, J. T. and Zender, C. S.: Global impact of smoke aerosols from
25 landscape fires on climate and the Hadley circulation, *Atmos. Chem. Phys.*, 13, 5227–5241,
26 doi:10.5194/acp-13-5227-2013, 2013.
- 27 Tosca, M. G., Diner, D., Garay, M., and Kalashnikova, O.: Observational evidence of fire-
28 driven reduction of cloud fraction in tropical Africa, *J. Geophys. Res.*, 119, 8418–8432,
29 doi:10.1002/2014JD021759, 2014.
- 30 Tosca, M. G., Diner, D. J., Garay, M. J., and Kalashnikova, O. V.: Human-caused fires limit
31 convection in tropical Africa: First temporal observations and attribution, *Geophys. Res. Lett.*,
32 42, doi:10.1002/2015GL065063, 2015.
- 33 [Tsigradis, K., Daskalakis, N., Kanakidou, M., Adams, P. J., Artaxo, P., Bahadur, R.,](#)
34 [Balkanski, Y., Bauer, S. E., Bellouin, N., Benedetti, A., Bergman, T., Berntsen, T. K.,](#)
35 [Beukes, J. P., Bian, H., Carslaw, K. S., Chin, M., Curci, G., Diehl, T., Easter, R. C., Ghan, S.](#)
36 [J., Gong, S. L., Hodzic, A., Hoyle, C. R., Iversen, T., Jathar, S., Jimenez, J. L., Kaiser, J. W.,](#)
37 [Kirkevåg, A., Koch, D., Kokkola, H., Lee, Y. H., Lin, G., Liu, X., Luo, G., Ma, X., Mann, G.](#)
38 [W., Mihalopoulos, N., Morcrette, J.-J., Müller, J.-F., Myhre, G., Myriokefalitakis, S., Ng, N.](#)
39 [L., O'Donnell, D., Penner, J. E., Pozzoli, L., Pringle, K. J., Russell, L. M., Schulz, M., Sciare,](#)
40 [J., Seland, Ø., Shindell, D. T., Sillman, S., Skeie, R. B., Spracklen, D., Stavrakou, T.,](#)
41 [Steenrod, S. D., Takemura, T., Tiitta, P., Tilmes, S., Tost, H., van Noije, T., van Zyl, P. G.,](#)
42 [von Salzen, K., Yu, F., Wang, Z., Wang, Z., Zaveri, R. A., Zhang, H., Zhang, K., Zhang, Q.,](#)
43 [and Zhang, X.: The AeroCom evaluation and intercomparison of organic aerosol in global](#)
44 [models, *Atmos. Chem. Phys.*, 14, 10845–10895, doi:10.5194/acp-14-10845-2014, 2014.](#)

- 1 [Turpin, B. J. and Lim, H.-J.: Species contributions to PM_{2.5} mass concentrations: Revisiting](#)
2 [common assumptions for estimating organic mass, *Aerosol Sci. Tech.*, 36, 602–610, 2001.](#)
- 3 [Vakkari, V., Kerminen, V.-M., Beukes, J. P., Tiitta, P., van Zyl, P. G., Josipovic, M., Venter,](#)
4 [A. D., Jaars, K., Worsnop, D. R., Kulmala, M., and Laakso, L.: Rapid changes in biomass](#)
5 [burning aerosols by atmospheric oxidation, *Geophys. Res. Lett.*, 41, 2644–2651,](#)
6 [doi:10.1002/2014GL059396., 2014](#)
- 7 [Val Martin, M., Logan, J. A., Kahn, R. A., Leung, F.-Y. , Nelson, D. L. and Diner, D. J.:](#)
8 [Smoke injection heights from fires in North America: Analysis of 5 years of satellite](#)
9 [observations, *Atmos. Chem. Phys.*, 10, 1491–1510, doi:10.5194/acp-10-1491-2010, 2010.](#)
- 10 van der Werf, G. R., Randerson, J. T., Collatz, G. J., and Giglio, L.: Carbon emissions from
11 fires in tropical and subtropical ecosystems, *Global Change Biol.*, 9, 547–562, 2003.
- 12 van der Werf, G. R., Randerson, J. T., Giglio, L., Collatz, G. J., Kasibhatla, P. S., and
13 Arellano, A. F.: Interannual variability in global biomass burning emissions from 1997 to
14 2004, *Atmos. Chem. Phys.*, 6, 3423–3441, doi:10.5194/acp-6-3523-2006, 2006.
- 15 van der Werf, G. R., Randerson, J. T., Giglio, L., Collatz, G. J., Mu, M., Kasibhatla, P. S.,
16 Morton, D. C., DeFries, R. S., Jin, Y., van Leeuwen, T. T.: Global fire emissions and the
17 contribution of deforestation, savanna, forest, agricultural, and peat fires (1997-2009), *Atmos.*
18 *Chem. Phys.*, 10, 11707-11735, doi:10.5194/acp-10-11707-2010, 2010.
- 19 Ward, D. S., Kloster, S., Mahowald, N. M., Rogers, B. M., Randerson, J. T., and Hess, P. G.:
20 The changing radiative forcing of fires: global model estimates for past, present and future,
21 *Atmos. Chem. Phys.*, 12, 10857-10886, doi:10.5194/acp-12-10857-2012, 2012.
- 22 Wiedinmyer, C., Quayle, B., Geron, C., Belote, A., McKenzie, D., Zhang, X., O'Neill, S., and
23 Wynne, K. K.: Estimating emissions from fires in North America for Air Quality Modeling,
24 *Atmos. Environ.*, 40, 3419–3432, 2006.
- 25 Wiedinmyer, C., Akagi, S. K., Yokelson, R. J., Emmons, L. K., Al-Saadi, J. A., Orlando, J. J.,
26 and Soja, A. J.: The Fire INventory from NCAR (FINN): a high resolution global model to
27 estimate the emissions from open burning, *Geosci. Model Dev.*, 4, 625-641,
28 doi:10.5194/gmd-4-625-2011, 2011.
- 29 Yu, S., Eder, B., Dennis, R., Chu, S.-H. and Schwartz, S. E.: New unbiased symmetric
30 metrics for evaluation of air quality models, *Atmosph. Sci. Lett.*, 7: 26–34. doi:
31 10.1002/asl.125, 2006.
- 32 Zhang, X., Kondragunta, S., Ram, J., Schmidt, C., and Huang, H.-C: Near-real-time global
33 biomass burning emissions product from geostationary satellite constellation, *J. Geophys.*
34 *Res.*, 117, D14201 doi:10.1029/2012JD017459, 2012.
- 35 [Zhou, J. C., Swietlicki, E., Hansson, H. C., and Artaxo, P.: Submicrometer aerosol particle](#)
36 [size distribution and hygroscopic growth measured in the Amazon rain forest during the wet](#)
37 [season, *J. Geophys. Res.*, 107 \(D20\), 8055, doi:10.1029/2001JD000203, 2002.](#)

1 **Table 1.** Summary of biomass burning emission inventories used in this study: the Global Fire
2 Emissions Database version 3 (GFED3), the National Centre for Atmospheric Research Fire Inventory
3 version 1.0 (FINN1) and the Global Fire Assimilation System version 1.0 (GFAS1). For each emission
4 inventory, the total amounts of black carbon (BC) and organic carbon (OC) aerosol emitted from fires
5 over the tropical region (defined as 23.5°N to 23.5°S) are given for the 2003 to 2011 average.
6 Numbers in parenthesis give the ratio to GFED3 emissions.

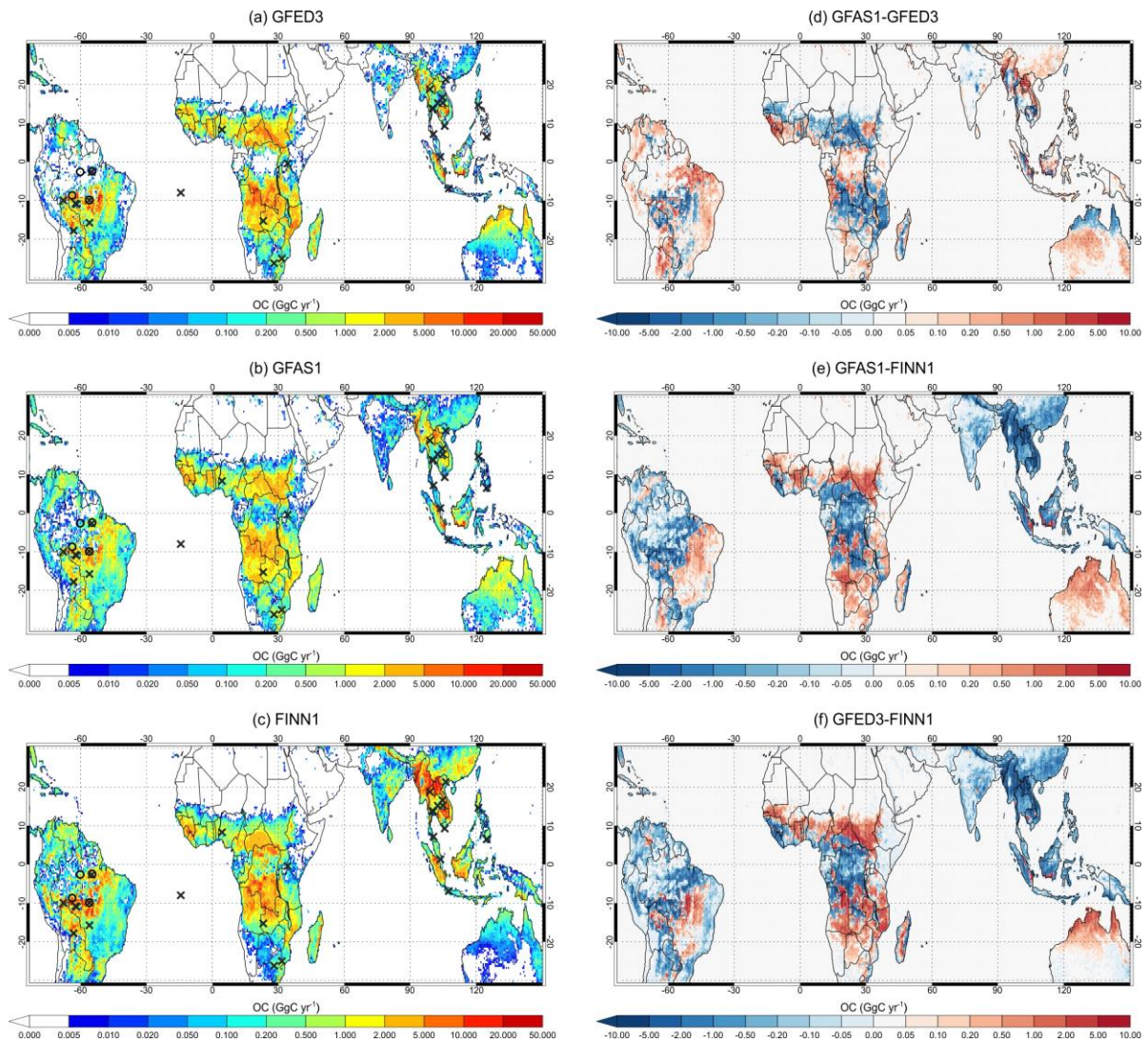
	GFED3	GFAS1	FINN1
Method	MODIS burned area & biogeochemical model	MODIS thermal anomaly product & fire radiative power	MODIS thermal anomaly product & assumed burned area
Spatial resolution	0.5° x 0.5°	0.5° x 0.5°	1 km x 1 km
Temporal resolution	Monthly (1997 – 2011) Daily (2003 – 2011)	Daily (2001 – 2015)	Daily (2002 – 2013)
Amount of OC emitted over tropics (Tg yr⁻¹)	13.412	11.731 (0.87)	17.282 (1.29)
Amount of BC emitted over tropics (Tg yr⁻¹)	1.705	1.532 (0.90)	1.724 (1.01)
OC:BC ratio over tropics	7.87	7.66	10.02
Reference	Van der Werf et al., 2010	Kaiser et al., 2012	Wiedinmyer et al., 2011

1 **Table 2.** Summary of scaling factors applied in previous modelling studies to biomass burning
2 emissions or modelled concentrations of biomass burning aerosol to match observations. Region
3 abbreviations used in the table are defined in van der Werf et al. (2006): Northern Hemisphere South
4 America (NHSA), Southern Hemisphere South America (SHSA), Northern Hemisphere Africa
5 (NHAF), Southern Hemisphere Africa (SHAF), Southeast Asia including the Philippines (SEAS) and
6 Equatorial Asia (EQAS). See van der Werf et al. (2006; 2010) for discussion of differences between
7 GFED versions 1, 2 and 3; on average GFED3 are 13% lower than GFED2 van der Werf et al. (2010),
8 with total GFED2 emissions lower than GFED1 in Central and Southern America and Southern Africa
9 (van der Werf et al., 2006).

10

Reference	Biomass burning emission inventory	Region of focus	Details of scaling applied
Myhre et al., 2003	Biomass burning BC emissions from the Global Emissions Inventory Activity (GEIA), based on Cooke and Wilson (1996); OC emissions from Lioussé et al. (1996).	<u>Southern Africa</u>	Used a relatively high OM/OC ratio of 2.6 and increased the modelled aerosol mass by 20% to account for mass fraction of inorganic components observed to be of 17% of the total mass.; focussing on southern Africa.
Matichuk et al., 2007	GFED1 (van der Werf et al., 2003)	<u>Southern Africa</u>	Multiple sensitivity studies were performed with the model including simulations with halved and doubled fire emissions.; focussing on southern Africa.
Matichuk et al., 2008	GFED2 (van der Werf et al., 2006)	<u>South America</u>	Smoke source function was scaled up by a factor of 6.; focussing on South America.
Johnson et al., 2008	Biomass burning emissions following Dentener et al. (2006): GFED1 (van der Werf et al., 2004) for year 2000 or a 5-year (1997–2001) average (not specified)	<u>West Africa</u>	Increased mass concentration of biomass burning AOD by a factor of 2.4.; focussing on West Africa.
Chin et al., 2009	Calculated using dry mass burned dataset from GFED2 (van der Werf et al., 2006)	<u>Global</u>	No scaling applied, but used <u>emission factor</u> EFs of BC (1 g kg ⁻¹) and OC (8 g kg ⁻¹) that are 40–100% higher than commonly used values (Andreae and Merlet, 2001).
Sakaeda et al., 2011	Aerosol fields taken from MATCH chemical transport model	<u>Southern Africa</u>	OC and BC masses were increased by a factor of 2 over 10°N–30°S and 20°W–50°E; focussing on southern Africa.
Johnston et al., 2012	GFED2 (van der Werf et al., 2006)	<u>Global</u>	Scalar adjustments made for 14 continental scale regions: NHSA (2.48-2.7), SHSA (1.9-3.3), NHAF (1.02-1.08), SHSA (1.68-2.01), SEAS (2.43-3.08), EQAS (2.3-2.72). Scaling factors were applied to modelled surface fire PM2.5 to match satellite observations of AOD (non-fire aerosol was also scaled).

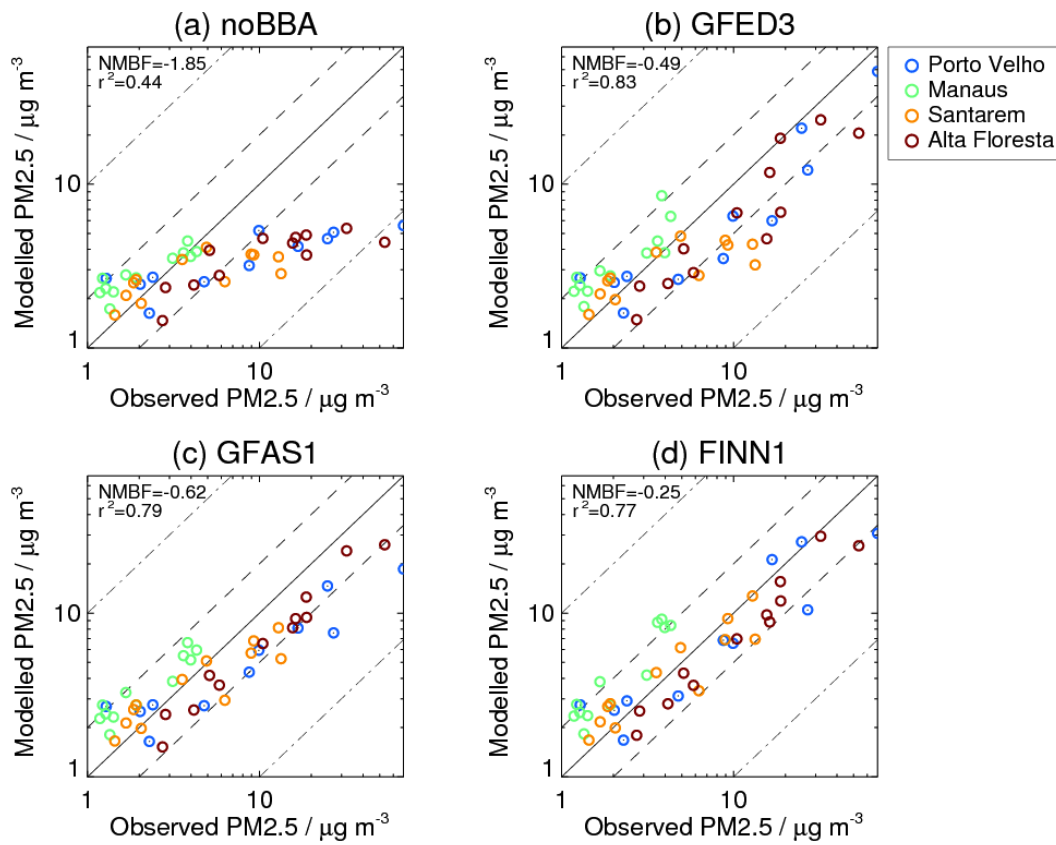
Kaiser et al., 2012	GFED3 and GFASv1.0	<u>Global</u>	Model was biased low in South America and Africa by factors of 4.1 and 3.0. Recommended a global enhancement of 3.4 for PM emissions from fires.
Ward et al., 2012	Calculated from Kloster et al. (2010, 2012) CLM3 simulations of global fire area burned; using emission factors from Andreae and Merlet (2001) and updates from Hoelzemann et al. (2004). Compared against GFED2.	<u>Global</u>	Scalar adjustments were made for continental scale regions following Johnston et al. (2012) with slight modifications: SHSA (2.0), NHAF (1.0), SHAF (3.0), SEAS (1.5), EQAS (3.0). Scaling factor directly applied to model fire emissions.
Tosca et al., 2013	GFED3	<u>Global</u>	Biomass burning BC and OC emissions scaled by factor of 2 globally with additional regional scaling factors applied: South America (2.4), Africa (2.1), Southeast Asia (1.67).
Marlier et al., 2013	GFED3	<u>Southeast Asia</u>	Total aerosol burden scaled by 1.02-1.96 (depending on model), with additional scaling factors of 1.36-2.26 applied to fire aerosol. focussing on <u>Southeast Asia.</u>



1

2 **Figure 1.** (a)-(c) Total annual emissions of organic carbon (OC) in Gg(C) yr⁻¹ averaged over the
 3 period of January 2003 to December 2011 from (a) GFED3, (b) GFAS1 and (c) FINN1. Black circles
 4 mark the locations of the four aerosol measurement stations and black crosses mark the locations of
 5 the 27 AERONET stations (see Table S1). (d)-(f) Absolute difference in 2003-2011 mean annual OC
 6 emissions between GFAS1, GFED3 and FINN1 (d) GFAS1 minus GFED3 (e) GFAS1 minus FINN1
 7 (f) GFED3 minus FINN1. The FINN1 OC emissions (with a 1 km x 1 km horizontal resolution) were
 8 aggregated onto a grid of 0.5° x 0.5° degree resolution to compare with GFED3 and GFAS1.

9

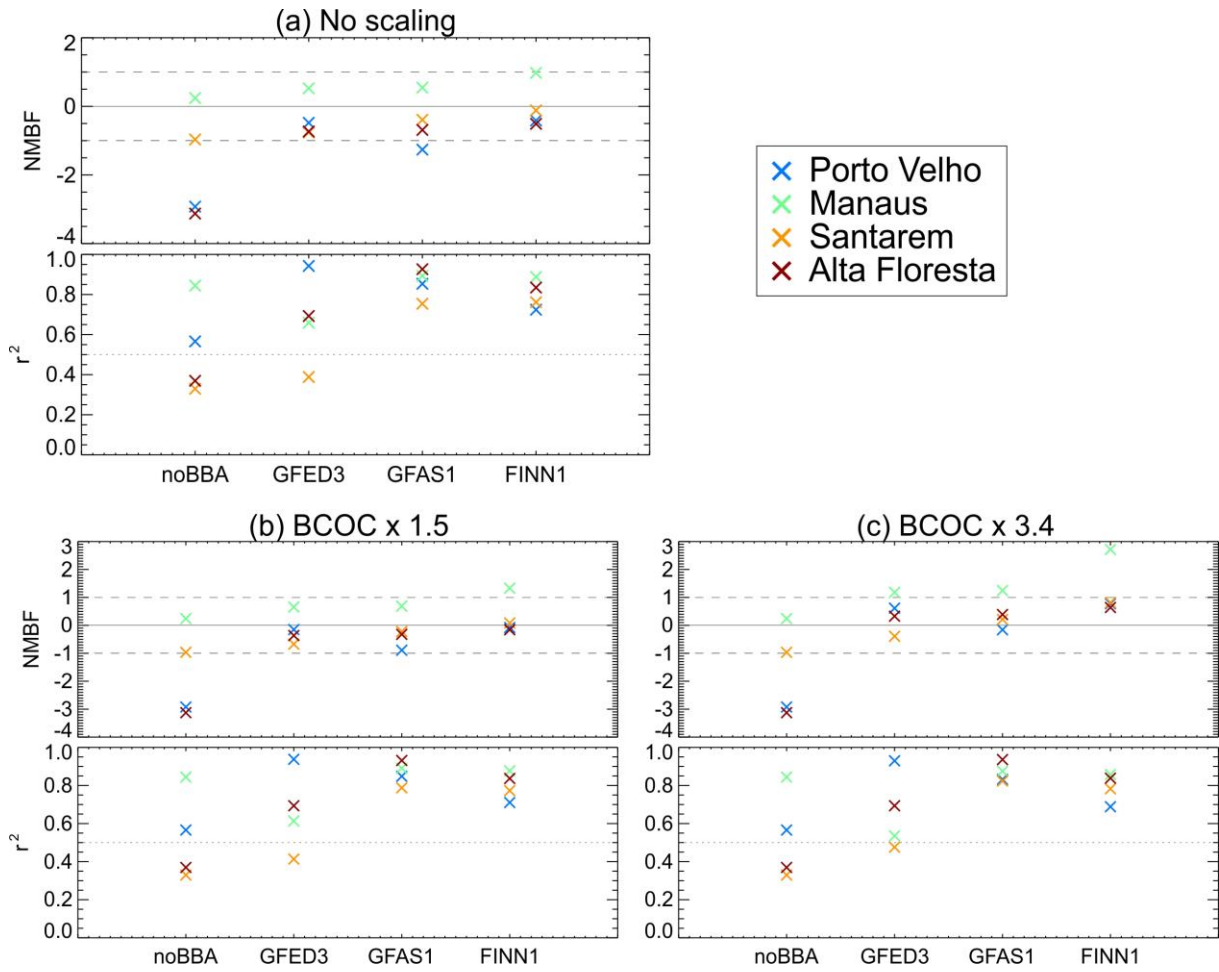


1

2 **Figure 2.** Simulated versus observed multi-annual monthly mean PM_{2.5} concentrations at each
 3 ground station in the Amazon region for the model (a) without biomass burning emissions, and with
 4 (b) GFED3, (c) GFAS1 and (d) FINN1 emissions. Multi-annual monthly mean concentrations were
 5 calculated by averaging over all years of data available between January 2003 and December 2011 to
 6 obtain an average seasonal cycle at each station. The normalised mean bias factor (NMBF; Yu et al.,
 7 2006) and Pearson's correlation (r^2) between modelled and observed PM_{2.5} concentrations are shown
 8 in the top left corner.

9

1



2

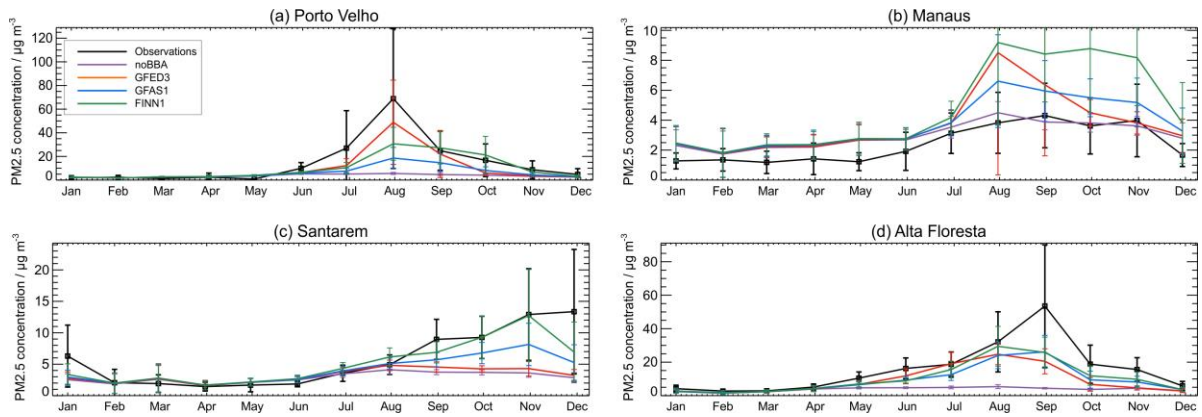
3 **Figure 3.** Normalised mean bias factor (NMBF; Yu et al., 2006) and Pearson's correlation coefficient
4 (r^2) between modelled and observed multi-annual monthly-mean PM_{2.5} concentrations at each of the
5 four ground stations in Amazonia. Results are shown for four model simulations: without fires
6 (noBBA), and with each of the three biomass burning emissions inventories: GFED3, GFAS1, FINN1.

7 (a) No scaling applied to the fire emissions; (b) particulate (BC/OC) fire emissions scaled up globally
8 by a factor 1.5; (c) particulate (BC/OC) fire emissions scaled up globally by a factor of 3.4. The

9 dashed lines indicate NMBFs of -1 and 1, which equate to an underestimation and overestimation,
10 respectively, of a factor of 2. The dotted line indicates an r^2 value of 0.5.

11

12



1

2

3

4

5

6

7

8

9

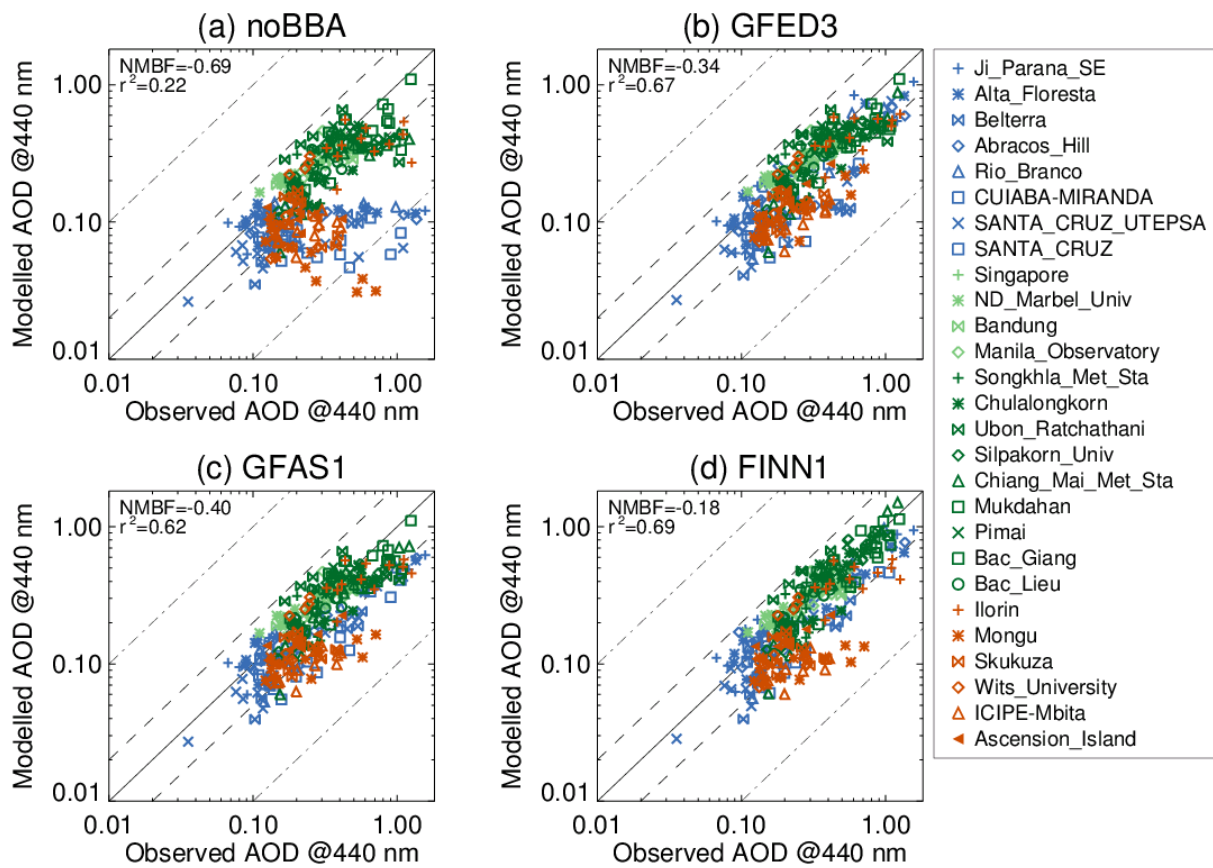
10

11

12

13

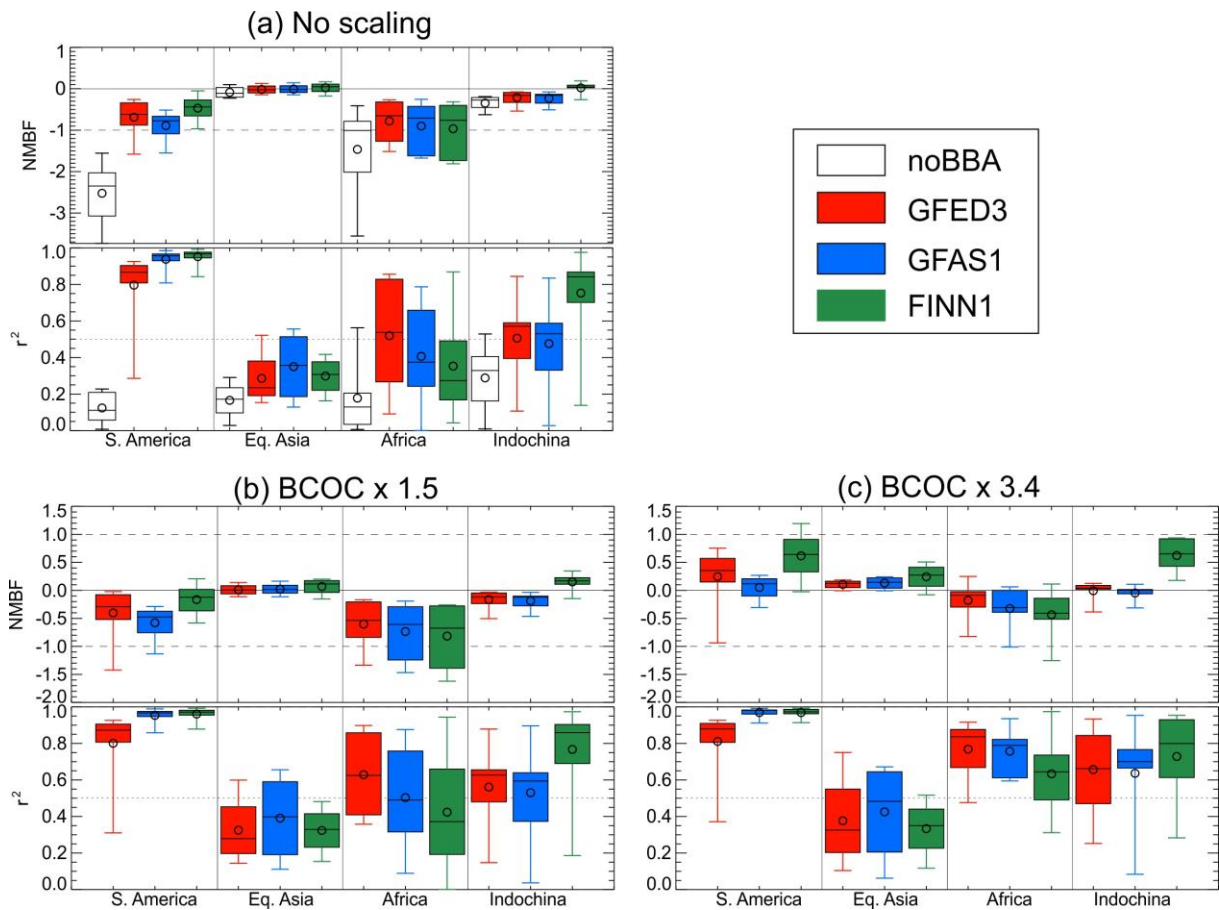
Figure 4. Average seasonal cycles in observed (black) and simulated (colour) multi-annual monthly mean PM_{2.5} concentrations at four ground stations in the Amazon region: **(a)** Porto Velho (2009-2011); **(b)** Manaus (2008-2011); **(c)** Santarem (2003-2006); and **(d)** Alta Floresta (2003-2004). Multi-annual monthly mean concentrations were calculated by averaging over all years of available observation data between January 2003 and December 2011. The modelled results are shown for four simulations: without biomass burning (purple), with GFED3 emissions (red), with GFAS1 emissions (blue) and with FINN1 emissions (green). The error bars show the standard deviation of the mean of the observed and simulated values, which represents the inter-annual and intra-monthly variability in the daily mean PM_{2.5} concentrations.



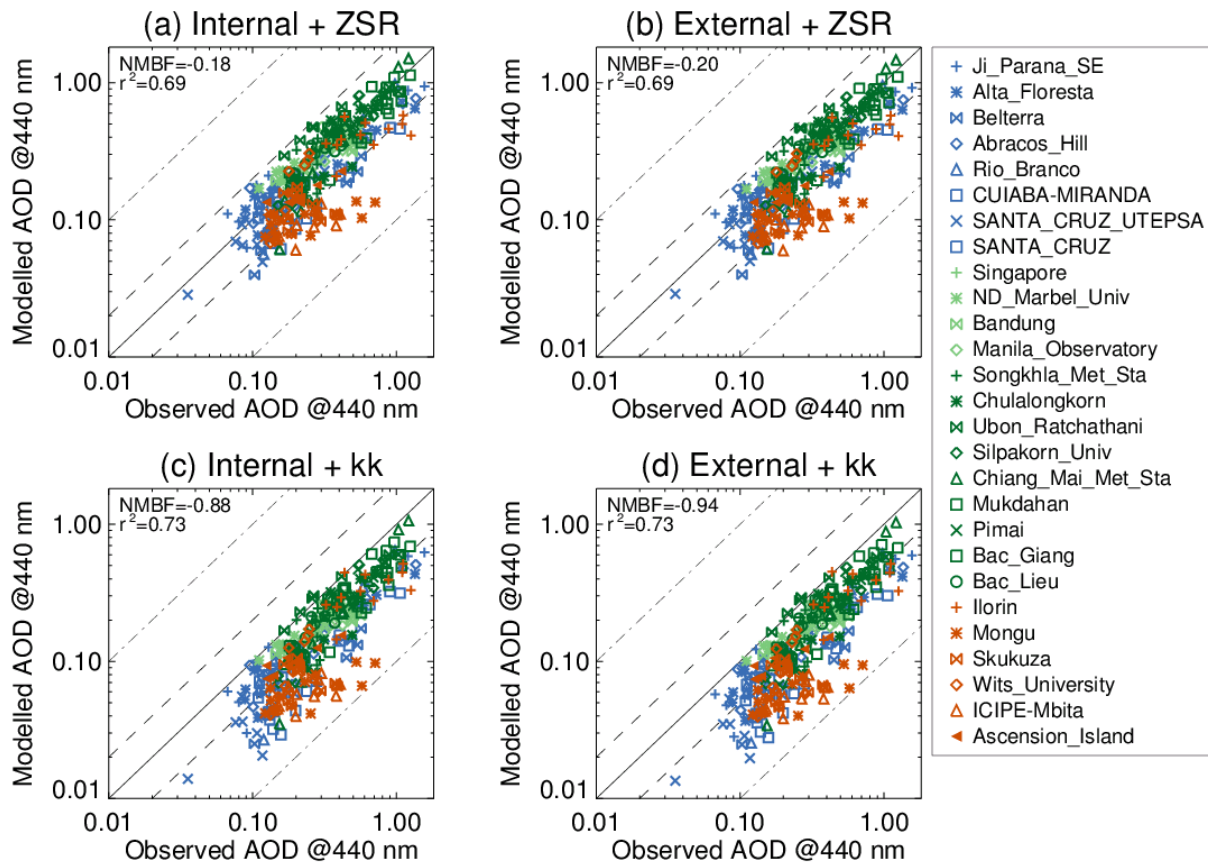
1

2 **Figure 5.** Simulated versus observed multi-annual monthly mean AOD at 440 nm at each AERONET
 3 station. The model is shown (a) without biomass burning emissions, and with (b) GFED3, (c) GFAS1
 4 and (d) FINN1 emissions. As for Fig. 2, the multi-annual monthly mean AODs were calculated using
 5 all years of daily mean data available between January 2003 and December 2011 to obtain an average
 6 seasonal cycle at each station. AERONET stations located in South America are shown in blue;
 7 stations in Southeast Asia are shown in green (stations in Equatorial Asia and Indochina in light and
 8 dark green, respectively); and stations in Africa are shown in orange. The normalised mean bias factor
 9 (NMBF) and Pearson's correlation (r^2) between modelled and observed PM_{2.5} concentrations are
 10 shown in the top left corner.

11

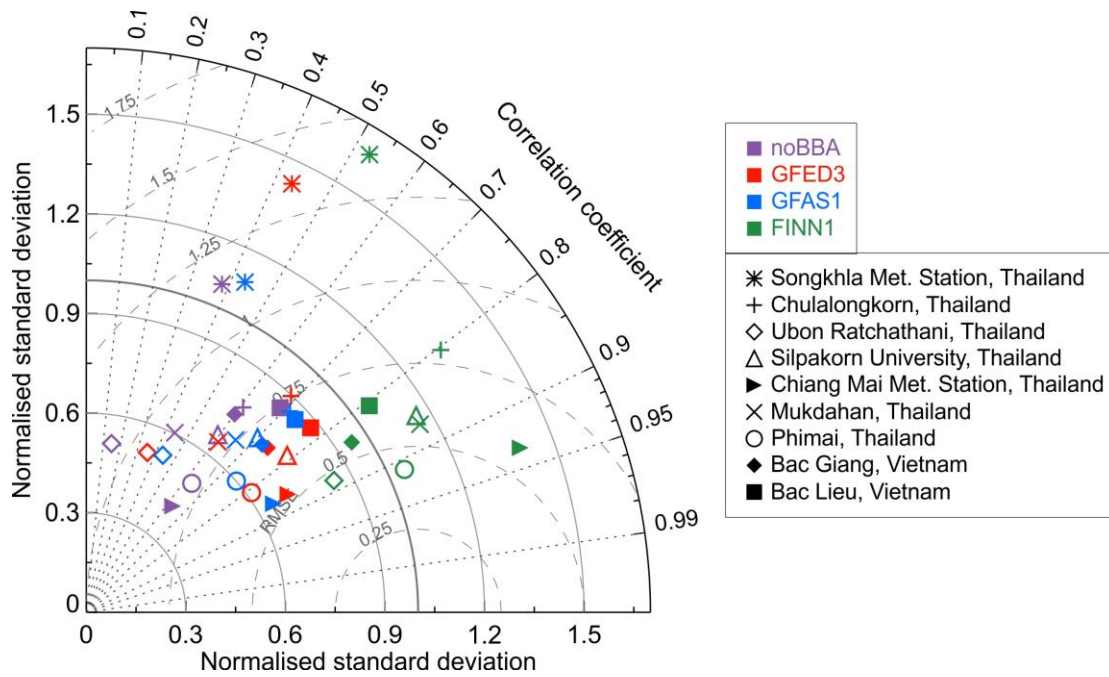


1
2 **Figure 6.** Box and whisker plots of the normalised mean bias factor (NMBF) and Pearson's
3 correlation coefficient (r^2) between modelled and observed multi-annual monthly-mean AOD at 440
4 nm for AERONET stations located in South America (8 sites), Equatorial Asia (4 sites), Africa (6
5 sites) and Indochina (9 sites). Results are shown for four model simulations: without fires (white), and
6 with each of the three biomass burning emissions inventories: GFED3 (red), GFAS1 (blue), FINN1
7 (green). (a) No scaling applied to the fire emissions; (b) particulate (BC/OC) fire emissions scaled up
8 globally by a factor 1.5; (c) particulate (BC/OC) fire emissions scaled up globally by a factor of 3.4.
9 The dashed lines indicate NMBFs of -1 and 1, which equate to an underestimation and overestimation,
10 respectively, of a factor of 2. The dotted line indicates an r^2 value of 0.5.



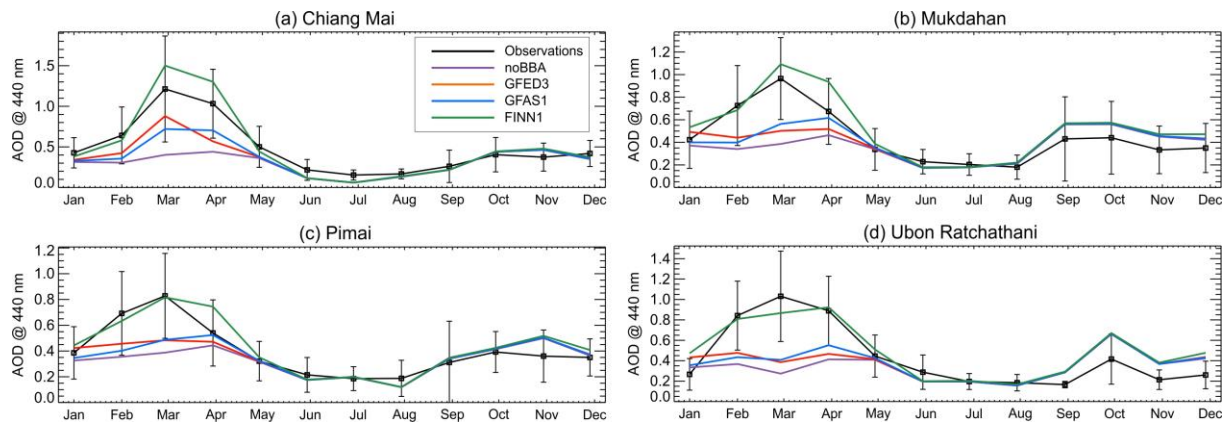
1
2
3
4
5
6
7
8
9
10
11

Figure 7. Simulated versus observed multi-annual monthly mean AOD at 440 nm at each AERONET station to demonstrate the sensitivity of simulated AOD to different assumptions. The model is with FINN1 fire emissions and simulated AOD is calculated assuming (a) internal mixing with ZSR water uptake scheme (identical to Fig. 5d), (b) external mixing with ZSR water uptake scheme, (c) internal mixing with κ -Köhler water uptake scheme, and (d) external mixing with κ -Köhler water uptake scheme. AERONET stations located in South America are shown in blue; stations in Southeast Asia are shown in green (stations in Equatorial Asia and Indochina in light and dark green, respectively); and stations in Africa are shown in orange. The normalised mean bias factor (NMBF) and Pearson's correlation (r^2) between modelled and observed PM_{2.5} concentrations are shown in the top left corner.



1
 2 **Figure 87.** Taylor diagrams (Taylor, 2001) comparing monthly mean modelled and observed AOD
 3 (440 nm) at 9 AERONET stations located in Indochina. The modelled and observed monthly mean
 4 AODs were calculated for every month with available daily mean data between January 2003 and
 5 December 2011. The observations are represented by a point on the x-axis at unit distance from the y-
 6 axis. The results are shown for four simulations: without biomass burning (purple), and with GFED3
 7 (red), GFAS1 (blue) and FINN1 (green) fire emissions. The model standard deviation and root mean
 8 square error (RMSE) are normalised by dividing by the corresponding observed standard deviation.
 9 The normalised standard deviation and RMSE values are marked by the grey-solid and grey-dashed
 10 lines respectively. The correlation coefficient (r) values are marked by the grey dotted lines.

11
 12
 13
 14
 15
 16



1
2
3
4
5
6
7
8
9

Figure 89. Average seasonal cycles in observed (black) and simulated (colour) monthly mean AOD at 440 nm at ~~three~~four AERONET stations in the Thailand: **(a)** Chiang Mai Met. Station; **(b)** Mukdahan; **(c)** Phimai; and **(d)** Ubon Ratchathani. Multi-annual monthly mean concentrations were calculated by averaging over all years of available daily mean observation data between January 2003 and December 2011. The modelled results are shown for four simulations: without biomass burning (purple), and with GFED3 (red), GFAS1 (blue) and FINN1 (green) fire emissions. The error bars show the standard deviation of the mean of the observations.